

Repairing Property Graphs under PG-Constraints

Christopher Spinrath
 Lyon 1 University, Liris CNRS
 Lyon, France
 christopher.spinrath@liris.cnrs.fr

Angela Bonifati
 Lyon 1 University, Liris CNRS & IUF
 Lyon, France
 angela.bonifati@univ-lyon1.fr

Rachid Echahed
 CNRS LIG, Univ. Grenoble Alpes
 Grenoble, France
 rachid.echahed@imag.fr

ABSTRACT

Recent standardization efforts for graph databases lead to standard query languages like GQL and SQL/PGQ, and constraint languages like Property Graph Constraints (PG-Constraints). In this paper, we embark on the study of repairing property graphs under PG-Constraints. We identify a significant subset of PG-Constraints, encoding denial constraints and including recursion as a key feature, while still permitting automata-based structural analyses of errors. We present a comprehensive repair pipeline for these constraints to repair Property Graphs, involving changes in the graph topology and leading to node, edge and, optionally, label deletions. We investigate three algorithmic strategies for the repair procedure, based on Integer Linear Programming (ILP), a naive, and an LP-guided greedy algorithm. Our experiments on various real-world datasets reveal that repairing with label deletions can achieve a 59% reduction in deletions compared to node/edge deletions. Moreover, the LP-guided greedy algorithm offers a runtime advantage of up to 97% compared to the ILP strategy, while matching the same quality.

Related Version:

This paper, without the appendix, has been accepted for publication in Volume 19 of PVLDB and will be presented at the 52nd International Conference on Very Large Data Bases (VLDB 2026).

Artifact Availability:

The source code, data, and/or other artifacts have been made available at <https://doi.org/10.5281/zenodo.18301604>.

1 INTRODUCTION

Repairing errors and inconsistencies is an elemental task when working with large datasets. Applications arise naturally as part of data integration scenarios or if requirements – e.g., the schema – of databases change. Consequently, error repairing has been studied extensively in the literature, for various database models [13].

Property graph languages spanning query languages, i.e. GQL and SQL/PGQ [18, 30], and schema and constraint languages, e.g. PG-Schema and PG-Keys [3, 4], have recently been standardized.

To the best of our knowledge, repairing techniques for property graphs under these schema and constraint languages have not been investigated yet. We embark on the study of *qualitative* error repairing [13] for *property graphs*, that is, error repairing with respect to *constraints*; or more precisely, a subset of PG-Constraints [3, 4], which are part of the PG-Schema formalism and extend PG-Keys.

Copyright ©2026 Christopher Spinrath, Angela Bonifati, and Rachid Echahed

This work is licensed under a [Creative Commons “Attribution-NonCommercial-NoDerivatives 4.0 International” license](#).



To motivate our work, we illustrate property graphs and PG-Constraints by means of a running example.

Example 1.1. Figure 1 depicts the property graph G_e modelling an organisation with persons, tasks, and documents for planning activities. Persons can work on tasks, which reference documents required for the task. Both, nodes and edges, can have multiple labels, and can be equipped with key-value pairs, called *properties*. For instance, the node d_3 has the two labels *document* and *important*, as well as the two properties *#pages* and *access_level*. Let us consider the following constraint for the property graph G_e .

“If a person works on a task, which has started and which references directly or indirectly, i.e. recursively, an important document, then the person’s access level is at least as high as the (required) access level of the referenced document.”

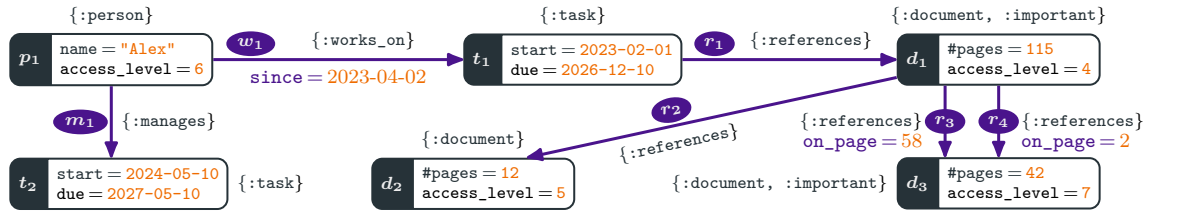
The constraint describes a *graph pattern* in its precondition: The part “a person works on a task” refers to a node labelled person and a node labelled task which are connected by an edge labelled *works_on*. A *match* of this partial pattern in G_e consists of the nodes p_1, t_1 , and the edge w_1 . The described pattern also extends to documents which are referenced – directly or indirectly – by the task. The match for the partial pattern above could be extended in several ways: d_1, d_2 , and d_3 are all documents referenced by t_1 , where d_2 and d_3 are referenced indirectly. In general, reference chains might be of arbitrary length. However, the document d_2 is not labelled *important* and thus it should not be matched.

Lastly, the constraint compares property values, namely the *start* property of t_1 to assert that the task has started, and the *access_level* properties of p_1 and, depending of which node is matched, d_1 or d_3 . A possible specification of this constraint as a *PG-Constraint* [4] is illustrated in Figure 1.

G_e violates the above constraint since $p_1, w_1, t_1, r_1, d_1, r_4$, and d_3 (with d_3 being the important document in question) form a match, the task t_1 has started, but d_3 has a higher access level than p_1 .

Contributions. We identify *regular graph pattern calculus (RGPC)* *constraints* as a subset of PG-Constraints, and introduce an automata model for its patterns to reason about the structure of errors. At the same time, our subset entails major features of PG-Constraints; especially, recursion, complex restrictions of labels for nodes and edges, as well as comparability of node properties. They can express denial constraints, which capture, among others, functional dependencies, including the constraint from Example 1.1. For specifying patterns we use a subset of the graph pattern calculus GPC [26], which captures the core features for patterns in GQL and SQL/PG.

For repairing databases various repair models have been studied in the literature [20], including the addition of new data [5], changing data values [8, 34, 43] – i.e. values of properties – and deletion [12]. The choice of a repair model depends on the setting.



PG-Constraint in GQL

```
FOR x, y MATCH z = (x:person)-[:works_on]->(u:task)(-[:references]->(:document))+(y:document & important) FILTER u.start <= NOW()
MANDATORY x.access_level, y.access_level FILTER x.access_level >= y.access_level
```

Figure 1: A property graph modelling an organisation with persons, tasks, and documents, along with a PG-Constraint

In this paper, we assume the repair model of deletions [see, e.g. 12, 20, 33] in which property graphs are repaired by deleting objects from it, i.e. nodes, edges, or labels. Deletions make sense as a repair model in several applications where inserting new data is undesirable or too risky, for example, due to privacy or security reasons. More concretely, in a social network inserting a friendship could expose private data, but deleting one can be rectified. In a property graph modelling a supply chain, inserting a sourced_from relationship between a manufacturer and a product which the manufacturer cannot actually supply can be disastrous for a company, while deleting such a relationship would highlight the issue of unavailability. In a scenario as modelled by the property graph shown in Figure 1, increasing, that is changing, the access level of a person or document is a security risk. Recall that the property graph shown in Figure 1 does not satisfy the constraint from Example 1.1, since the person represented by p_1 works on the task t_1 which references the important document d_3 . But the access level of p_1 is not high enough to access d_3 . One way to repair the property graph is to delete the edge w_1 , effectively removing p_1 from working on t_1 . Another possibility is to remove the label `important` from d_3 .

In this paper, we propose a comprehensive pipeline (cf., Figure 2) featuring different graph repair options. The repair method follows a *holistic* approach, meaning it detects and repairs all errors simultaneously. This ensures that the fewest possible objects are removed, and their relationships are respected: For example, the deletion of a node entails deleting all its incident edges. However, managing multiple errors – especially those involving long, arbitrary-length paths rather than fixed-length tuples – can be time-consuming. To mitigate this, we propose three algorithms for tackling the underlying combinatorial problem of determining which objects to delete. The first is a naive greedy algorithm, which sequentially repairs each error by deleting an object from it, unless it has already been resolved through prior deletions. The second formulates the problem as an integer linear program (ILP), using a solver to derive an optimal set of objects for deletion. The third one is an LP-guided greedy algorithm which uses non-integer solutions of the LP-relaxation of the ILP to guide the greedy algorithm.

Finally, we gauge the effectiveness of our repair pipeline and analyse the trade-offs associated with the different algorithms and options through experiments conducted on real-world datasets. They reveal that the LP-guided greedy algorithm can outperform the other algorithms, while maintaining the quality, i.e. number of

deletions, of the ILP strategy. Permitting label deletions can reduce the number of deletions by up to 59%, but increases the runtime (by up to 5 \times). Moreover, our experiments reveal that approximate versions of our algorithms can be up to 89% faster, while yielding a good approximation or even a repair.

Structure. In Section 2 we recall some basics on property graphs, and present our subset of the graph pattern calculus (GPC). We then introduce our RGPC constraints in Section 3. In Section 4 we present our pipeline and algorithm(s) for error repairing, and in Section 5 our experiments. Finally, we discuss further related work in Section 6, and conclude in Section 7.

2 PRELIMINARIES

In this section, we provide basics on the data model used in property graphs, and introduce the subset of the pattern calculus GPC [26] which we use as an ingredient for our constraints in Section 3.

2.1 Property Graphs

By \mathcal{L} , \mathcal{K} , \mathcal{V} , and \mathcal{I} we denote countably infinite, pairwise disjoint sets of *labels*, *keys* (of properties), *property values*, and *identifiers* (*ids* for short), respectively.

A *property graph* is a tuple $G = (N, E, \rho, \lambda, \pi)$, where

- $N \subset \mathcal{I}$ is a finite set of node identifiers;
- $E \subset \mathcal{I}$ is a finite set of edge identifiers disjoint from N ;
- $\rho: E \rightarrow (N \times N)$ defines the endpoints, i.e. the source and target, for all edges;
- $\lambda: (N \cup E) \rightarrow 2^{\mathcal{L}}$ is a labelling function that assigns a finite set of labels to node and edge identifiers; and
- $\pi: ((N \cup E) \times \mathcal{K}) \rightarrow \mathcal{V}$ is a partial function assigning values to pairs of (node or edge) identifiers and keys.

For convenience, we will refer to node and edge identifiers simply as the *nodes* and *edges* of the property graph. Also, we use the term *object* to refer to nodes, edges, and labels on specific nodes or edges.

For example, the nodes of the property graph G_e depicted in Figure 1 are $p_1, t_1, t_2, d_1, d_2, d_3$ and the edges are $w_1, m_1, r_1, r_2, r_3, r_4$. The endpoints of the edge w_1 are p_1 (the source) and t_1 (the target). We note that it is possible that a node or an edge does not have any labels. In that case, λ assigns the empty set (of labels).

A *path* in a property graph $G = (N, E, \rho, \lambda, \pi)$ is a non-empty alternating sequence $v_0e_1v_1 \dots e_nv_n$ where $v_0, \dots, v_n \in N$ are nodes and $e_1, \dots, e_n \in E$ are edges such that $\rho(e_i) = (v_{i-1}, v_i)$ holds for all

$i \in \{1, \dots, n\}$. For example, the sequence $p_1 w_1 t_1 r_1 d_1 r_3 d_3$ is a path in G_e . We emphasize that every path starts and ends with a node. The *length* of a path $v_0 e_1 v_1 \dots e_n v_n$ is the number of edges n . An empty path consists of exactly one node and has length 0. Two paths $v_0 e_1 \dots e_n v_n$ and $v'_0 e'_1 \dots e'_m v'_m$ can be *concatenated* if $v_n = v'_0$ holds. The resulting path is then $v_0 e_1 \dots e_n v_n e'_1 \dots e'_m v'_m$. The *trace* $\lambda(P)$ of a path $P = v_0 e_1 v_1 \dots e_n v_n$ is $\lambda(P) = \lambda(v_0) \lambda(e_1) \lambda(v_1) \dots \lambda(e_n) \lambda(v_n)$. For example, the trace of the path $p_1 w_1 t_1 r_1 d_1 r_3 d_3$ is

```
{person}{works_on}{task}{references}
{document, important}{references}{document, important}.
```

2.2 Regular Graph Pattern Calculus

In the following we introduce the syntax and semantics of a proper subset of GPC, a graph pattern calculus, which captures the core features of the pattern sublanguage shared by GQL and SQL/PGQ [26]. We present our subset, which we call RGPC (short for *regular GPC*), by means of examples.

Example 2.1. The following RGPC pattern matches all pairs x, y of nodes such that x has the label *document* and there is a path z from x to y on which every edge has the label *references*.

$$z = (x : \text{document}) [\xrightarrow{\text{:references}}]^* (y)$$

We explain the components of the pattern in Example 2.1, as well as some variations, in a bottom-up fashion. The basic building blocks of RGPC patterns are *node* and *edge patterns*. A node pattern has the form $(x : \varphi)$ where x is a *node variable* and φ is a *label expression* which restricts the labels of the nodes matching the pattern. Both x and φ are optional. The node patterns in Example 2.1 are $(x : \text{document})$, and (y) . In the latter pattern the labels of y are not restricted, the node may have any label(s). An example for a node pattern without variable is $(: a)$. If x and φ are both omitted, we just write $()$. In general, φ can be any propositional formula connecting labels from the set \mathcal{L} with the operators \wedge (conjunction), \vee (disjunction), and \neg (negation). For example, $(: (a \wedge b) \vee \neg c)$ matches every node which has labels a and b or not label c .

Similarly to node patterns, edge patterns have the form $\xrightarrow{\varphi}$, although we do not consider variables in edge patterns. In Example 2.1, there is one edge pattern, namely $\xrightarrow{\text{:references}}$.

Path Patterns. Node and edge patterns can be combined into *path patterns* using *concatenation*, *union*, and *repetition*.

For example, a *concatenation* of two node and an edge pattern is

$$(x : \text{document}) \xrightarrow{\text{:references}} (y)$$

which matches all pairs x, y of nodes such that x has the label *document* and there is an edge labelled *references* from x to y .

The *union* of two patterns can be built if they *do not contain node variables*. For instance, $\xrightarrow{a} \cup \xrightarrow{c} \xrightarrow{c}$ states that there is an edge labelled a , or a path of length two on which all edges are labelled c .

For *repetitions* we consider the classic Kleene-star operator. For example, $[\xrightarrow{a}]^*$ specifies that the path specified by \xrightarrow{a} can be repeated arbitrarily often (including 0 times). We also write $[\xrightarrow{a}]^+$ as shorthand for $\xrightarrow{a} [\xrightarrow{a}]^*$. Similar to union, repetition is limited to patterns that do not contain any node variables. Additionally, patterns below a repetition must not match a path of length 0.

Of course, concatenation, union, and repetition can be nested. To improve readability (round brackets are used in node patterns) we use square brackets for disambiguation.

Graph Patterns. Finally, *graph patterns* are conjunctions of path patterns, associated with pairwise distinct *path variables*.¹ For example, the following graph pattern consists of two path patterns

$$z_a = (x : b) \xrightarrow{a} (y), z_c = (y) \xrightarrow{c} (x)$$

with variables z_a and z_c . It specifies that there are nodes x, y in the property graph such that x is labelled b , there is an edge (x, y) labelled a , and a path from y to x on which every edge is labelled c . Let us point out that path and node variables are disjoint.

Example 2.2. Consider the following graph pattern where p, w, t, d, r and i are shorthands for the labels *person*, *works_on*, *task*, *document*, *references* and *important*, respectively.

$$z = (x : p) \xrightarrow{w} (t : t) [\xrightarrow{r} (d : d)]^+ (y : d \wedge i)$$

It specifies the topology from Example 1.1: person x works on a task which (possibly indirectly) references an important document y . Note that all nodes on the subpath from the task to y must be labelled *document*, except for the first node, representing the task.

Semantics. A *match* for a (graph) pattern q in a property graph G is a mapping μ that maps the node and path variables of q to nodes and paths in G , respectively, which constitutes an answer to q on G . We refer to the literature [26] for a formal definition.

Example 2.3. A match for the pattern in Example 2.2 in the property graph depicted in Figure 1 is the mapping μ with $\mu(x) = p_1$, $\mu(y) = d_3$, and $\mu(z) = p_1 w_1 t_1 r_1 d_1 r_3 d_3$.

3 CONSTRAINTS FOR PROPERTY GRAPHS

With the preliminaries in place, we are now ready to introduce the constraints we study in this paper. We first explain the idea by means of an example, and then make the terms more precise.

Example 3.1. We consider the following constraint as a running example in this section: “Every document has a greater access level than any other document referenced (directly or indirectly) by it, that has not been edited since 2020.”

The core ingredient of a constraint is an RGPC graph pattern, incorporating characteristics of established graph query languages such as GQL and SQL/PGQ, notably recursion. This allows us to express the topology described in Example 3.1: The constraint affects all pairs of documents, say x and y , such that x references (directly or indirectly) y . The following RGPC pattern models this topology.

$$z = (x : \text{document}) [\xrightarrow{\text{:references}}]^+ (y : \text{document})$$

The RGPC pattern is complemented with two more ingredients to yield a constraint. Both ingredients can refer to node variables.

The first can be understood as an additional filter on the matches of the pattern. For instance, the predicate $x \neq y$ ensures that x and y in the above pattern are matched to different documents. Furthermore, the constraint in Example 3.1 only affects documents y which have not been edited since 2020. Assuming nodes labelled *document*

¹In the original definition of GPC, path variables are optional, but here they are obligatory. They also do not have to be distinct. We demand them to be distinct to avoid “hidden” path equality constraints.

have a property for the last time it was edited, i.e. a timestamp, this can be ensured by the predicate $y.\text{edited} \leq 2020-12-31$. In general, it is possible to supply any number of predicates (or none), in which case all of them have to hold for a match to pass the filter.

The last ingredient also consists of predicates and states which conditions have to hold, for every match of the pattern that passes the filter. For our example, the condition is the set consisting of the predicate $x.\text{access_level} \geq y.\text{access_level}$.

Overall the constraint described in Example 3.1 can be written as follows using the shorthands from Example 2.2.

$$\begin{aligned} z = (x:d) [\xrightarrow{\cdot r}]^+ (y:d); \{x \neq y, y.\text{edited} \leq 2020-12-31\} \\ \Rightarrow \{x.\text{access_level} \geq y.\text{access_level}\} \end{aligned}$$

In general, the constraints we study in this paper have the shape $q; F \Rightarrow C$ where q is an RGPC graph pattern, and F and C are sets of predicates modelling the filter and conditions of the constraint, respectively. More precisely, we consider all comparison predicates of GQL [30, Section 19.3]: $x_i = y_j$, $x_i \neq y_j$, $x_i.\text{propA} \oplus y_j.\text{propB}$, and $x_i.\text{propA} \oplus c$ where x_i and y_j are node variables that occur in q , $\oplus \in \{=, \neq, \leq, \geq, <, >\}$, and c is a value from \mathcal{V} .

The semantics of these predicates are as usual, with the noteworthy trait that all mentioned properties have to exist. For example, the filter and condition in the constraint above imply the existence of the `edited` and `access_level` property, respectively. A formal definition is available in Appendix A.2. A match μ satisfies a set of predicates if it satisfies all predicates in the set. A property graph G satisfies a constraint $q; F \Rightarrow C$ if every match μ in G for q satisfies C or not F .

Example 3.2. The following constraint σ is described informally in Example 1.1.

$$\begin{aligned} z = (x:p) \xrightarrow{\cdot w} (u:t) \underbrace{[\xrightarrow{\cdot r} (:d)]^+ (y:d \wedge i)}_q; \\ \{u.\text{start} \leq \text{now}\} \Rightarrow \{x.\text{access_level} \geq y.\text{access_level}\} \end{aligned}$$

Here q is the RGPC pattern explained in Example 2.2, except for the additional node variable u . We use “now” as a place holder for the current timestamp. The property graph illustrated in Figure 1 does not satisfy the constraint, because the match in Example 2.3 satisfies the filter (the start date of the task is in the past), but not $\{x.\text{access_level} \geq y.\text{access_level}\}$. Indeed, x is matched to p_1 and y to d_3 and we have $p_1.\text{access_level} = 6 \not\geq 7 = d_3.\text{access_level}$.

As discussed in the introduction, the constraint σ from Example 3.2 can be expressed as the PG-Constraint in Figure 1: The RGPC pattern is translated into a GQL, ASCII-art-like pattern, and the filter and consequence are expressed as `FILTER` clauses. Analogously, all RGPC constraints can be written as PG-Constraints.

Example 3.3. So far our examples were implication dependencies, a subclass of denial constraints. Using an unsatisfiable predicate like $x \neq x$, which we simply denote as `false`, we can also express denial constraints which do not fall into this subclass. For instance, the following denial constraint states that there are no cyclic references between documents.

$$(x:d) [\xrightarrow{\cdot r} (:d)]^+ (x); \emptyset \Rightarrow \{\text{false}\}$$

4 REPAIRING PROPERTY GRAPHS

This section is dedicated to the presentation of our repair pipeline, which is depicted in Figure 2. We start by introducing the notion of a *repair of a property graph* in Section 4.1. In Section 4.2 we present the *base pipeline*, that is, our pipeline without any of the optional steps it features. They are introduced in Sections 4.3 and 4.4.

4.1 Property Graph Repairs

As discussed in the introduction, motivated by applications where changing or adding objects is too risky due to, e.g. privacy or security reasons, we repair property graphs by deleting objects – i.e. nodes, edges, or labels – from it.

Example 4.1. Consider the property graph G_e depicted in Figure 1 and the constraint σ from Example 3.2. The property graph G_e does not satisfy the constraint, because “Alex” works on task t_1 which indirectly references, via document d_1 , the important document d_3 . However, “Alex” has a strictly smaller access level than d_3 .

To repair G_e , under the repair model of deletions, it suffices to delete one of the nodes p_1, t_1, d_1 , or d_3 , or one of the edges w_1 or r_1 between them. Note that deleting either r_3 or r_4 is not sufficient (but deleting both is). Moreover, all of these options will change the *topology* of G_e .

Another option is to delete a label of a node or edge, for instance, here it would suffice to remove the label `:important` from d_3 . This option does not change the topology of the graph at all.

To properly specify repairs, we will employ *subgraphs*. Intuitively, a subgraph is a property graph obtained by deleting nodes, edges, labels (or properties) from a given property graph.

Definition 4.2 (Subgraph). Let $G = (N, E, \rho, \lambda, \pi)$ be a property graph. A property graph $G' = (N', E', \rho', \lambda', \pi')$ is called a *subgraph* of G if the following five conditions hold: (i) $N' \subseteq N$, (ii) $E' \subseteq E$, (iii) $\rho'(o') = \rho(o') \cap (N' \times N')$ for all $o' \in E'$, (iv) $\lambda'(o') \subseteq \lambda(o')$ for all $o' \in N' \cup E'$ and (v) If $\pi'(o', k)$ is defined for a property key k and $o' \in N' \cup E'$, then so is $\pi(o', k)$ and $\pi'(o', k) = \pi(o', k)$. That is, all nodes, edges, labels, and properties (as well as their values) of G' are also present in G . If all nodes and edges in G' have exactly the same labels and property key/value pairs as in G , i.e. if $\lambda'(o') = \lambda(o')$ and $\pi'(o', k) = \pi(o', k)$, for all $o' \in N' \cup E'$ and property keys k , then we call G' a *topological subgraph* of G . We have that G' is a *proper subgraph* of G , if $G \neq G'$ holds.

For example, removing the label `:important` from node d_3 in the property graph G_e depicted in Figure 1 results in a proper subgraph, say G_e^* . The subgraph G_e^* is not topological because the node d_3 is also present in the original graph G_e but the labels of d_3 in G_e^* are not the same as in G_e . Another example is the topological subgraph obtained from G_e by deleting the edges r_3 and r_4 .

For being a *repair*, a subgraph has to satisfy all constraints, and, in the spirit of previous work [see, e.g. 12, Definition 2.2], it should be maximal, i.e. there should be no unnecessary deletions.

Definition 4.3 (Repair). Given a property graph G and a set Σ of constraints, a *repair* of G is a subgraph G' of G that

- satisfies Σ ; and
- is *maximal*, that is, there is no subgraph G'' of G such that G' is a proper subgraph of G'' and G'' satisfies Σ .

When a subgraph G_a of G satisfies Condition a) but not necessarily Condition b), we call G_a an *approximate* repair. A *topological (approximate) repair* is defined analogously to a(n approximate) repair, except that all subgraphs involved are topological subgraphs.

Example 4.4 (Continuation of Example 4.1). Let G'_e be the subgraph of the property graph G_e obtained by deleting the edge r_1 between t_1 and d_1 . We observe that G'_e is a topological repair. But it is *not* a repair, because the subgraph G''_e obtained from G_e by removing (just) the `:references` label from r_1 is also a repair, and G'_e is a subgraph of G''_e . Thus, Condition b) of Definition 4.3 is violated. It is, however, an approximate repair, since it satisfies Condition a).

Similarly, removing the node d_3 is not a repair, since it suffices to remove either the `:document` or the `:important` label. Observe that removing a node always implies removing all edges involving this node as well: otherwise, the result is not a well-defined property graph. Thus, the removal of d_3 leads to the removal of the edges r_3 and r_4 . But then the resulting subgraph is also *not* a topological repair: it is possible to add back d_3 , as long as the edges are not added back. We discuss this effect in more detail later on.

4.2 The Base Pipeline

We are now ready to present our repair pipeline, which is illustrated in Figure 2. It takes a set Σ of RGPC constraints and a property graph G as input, and has 6 steps, the last of which carries out the deletion operations. Two of these steps are optional, namely steps 2 and 3: they lead to label removals and a controllable trade-off between quality and runtime, respectively. In the following, we first discuss the *base pipeline*, consisting of steps 1, 4, 5, and 6.

Error Retrieval (Step 1). Intuitively, we understand an error as a set of objects witnessing that a constraint is not satisfied by the property graph. Since all path patterns of an RGPC constraint are associated with a path variable, an error can be obtained from the range of a match which satisfies the filter but not the consequence of the constraint.

Consider again the constraint from Example 3.2 and the property graph depicted in Figure 1. The property graph does not satisfy the constraint, because there are two matches of the constraint's pattern which pass the filter and do not satisfy the condition of the constraint: The first match corresponds to the path $p_1 w_1 t_1 r_1 d_1 r_3 d_3$ (cf. Example 2.3), and the second one to the path $p_1 w_1 t_1 r_1 d_1 r_4 d_3$. As illustrated in Figure 3 (1), (2), the sets of nodes and edges occurring on these paths, namely $O_1 = \{p_1, w_1, t_1, r_1, d_1, r_3, d_3\}$ and $O_2 = \{p_1, w_1, t_1, r_1, d_1, r_4, d_3\}$ constitute *topological errors*.

Definition 4.5 (Topological Error). Let $G = (N, E, \rho, \lambda, \pi)$ be a property graph, $q; F \Rightarrow C$ be a constraint with path variables z_1, \dots, z_k , and μ be a match for q in G that witnesses G *not* satisfying the constraint. The set O_μ , consisting of all nodes and edges, $o \in N \cup E$, for which there is an i , $1 \leq i \leq k$, such that o occurs in $\mu(z_i)$, is called a *topological error* of the constraint in G .

Error detection by means of graph queries has already been introduced in previous work [4]. We put this approach into practice and delegate error detection and retrieval to a graph database system by rewriting every constraint into an *error query*, which asks for all paths involved in an error. For example, the constraint from Example 3.2 is rewritten into the following GQL error query.

```

MATCH z = (x:person)-[:works_on]->(u:task)
      (-[:references]->(:document))+
      (y:document & important)
FILTER u.start IS NOT NULL AND u.start <= NOW()
AND (x.access_level < y.access_level
     OR x.access_level IS NULL OR y.access_level IS NULL)
RETURN z

```

Hypergraph Construction (Step 4). For repairing the property graph, the idea is to pick one object from each error and delete it. Since every error corresponds to a match, deleting a single object from it suffices to eliminate the match; hence, the resulting property graph satisfies the constraint(s). However, the outcome is not necessarily a repair. For instance, selecting r_1 and r_4 from the errors O_1 and O_2 discussed above, respectively, does not yield a repair, because it is possible to add r_4 back without violating the constraint. This is because r_1 occurs in both errors. We already discussed in Example 4.4 that removing nodes can have a similar effect.

To address this issue it helps to understand a collection of (topological) errors as a hypergraph, called *conflict hypergraph*. A *hypergraph* is a pair $\mathcal{H} = (\mathcal{W}, \mathcal{E})$ consisting of a set \mathcal{W} of vertices² and a set $\mathcal{E} \subseteq 2^\mathcal{W}$ of hyperedges. The conflict hypergraph for our running example is depicted in Figure 3 (3).

Definition 4.6 (Topological Conflict Hypergraph). Given a property graph $G = (N, E, \rho, \lambda, \pi)$, a set Σ of constraints, the *topological conflict hypergraph* of G w.r.t. Σ is the hypergraph $\mathcal{H} = (\mathcal{W}, \mathcal{E})$ whose edges are precisely all topological errors of all constraints in Σ in G , and where $\mathcal{W} = \bigcup_{O \in \mathcal{E}} O$ is the union of all these edges.

Computing a Repair (Step 5c). To repair a property graph, the idea is to select vertices from the conflict hypergraph with high-inbetweenness, i.e. vertices which participate in a high amount of errors. At the same time we want to select a minimal number of vertices. This amounts to computing a minimal vertex cover:

A *vertex cover* of a hypergraph $\mathcal{H} = (\mathcal{W}, \mathcal{E})$ is a set $V \subseteq \mathcal{W}$ such that $V \cap O \neq \emptyset$, for each $O \in \mathcal{E}$. A vertex cover V is minimal if there is no vertex cover V' with $V' \subsetneq V$.

Intuitively, a minimal vertex cover tells us which objects to delete to obtain a repair. For example, a vertex cover for the conflict hypergraph with hyperedges O_1 and O_2 from above is $V = \{r_1\}$. Trivially, no subset of V is a vertex cover, and removing r_1 yields a repair, as discussed above. The set $V \cup \{r_4\} = \{r_1, r_4\}$ is not a minimal vertex cover, since it contains V . And indeed, removing r_1 and r_4 does not yield a repair for the same reason: r_4 can be added (back).

However, this does not address the issue of node removal implying removal of incident edges. For instance, $\{d_3\}$ is a minimal vertex cover, but as discussed in Example 4.4, removing d_3 implies the removal of r_3 and r_4 , and does not yield a repair. Therefore, the deletion of nodes should be avoided, unless it is necessary, e.g. because an error consists only of nodes. We realize this by assigning a weight to each vertex of the conflict hypergraph \mathcal{H} . The weight $w(n)$ of a node n of the property graph is the number of edges incident to n plus one. The weight $w(e)$ of an edge e is simply 1. We are then interested in a *minimum weight vertex cover* [see e.g. 44] of \mathcal{H} . The weight of a vertex cover V is $w(V) = \sum_{v \in V} w(v)$. A *minimum weight vertex cover* V is a vertex cover whose weight $w(V)$ is the

²We call them vertices to differentiate them from the nodes of property graphs.

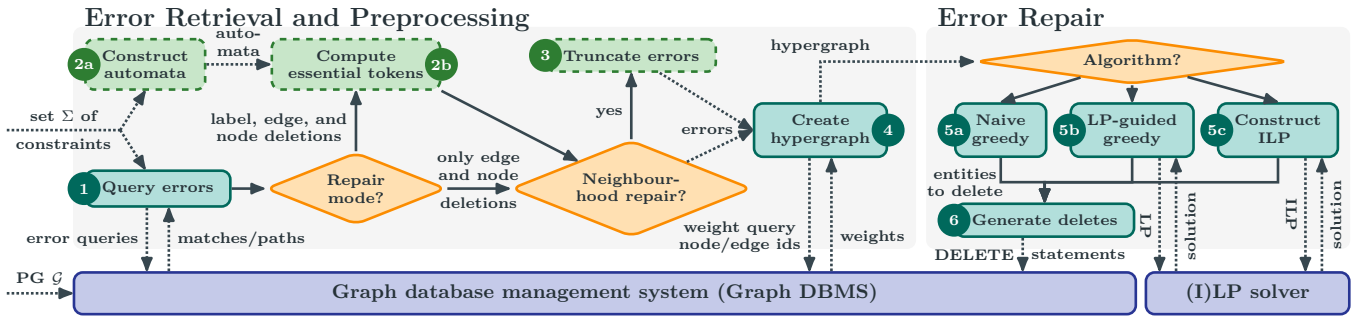


Figure 2: Our repair pipeline for property graphs consists of 6 steps, where steps 2 and 3 are optional. 2a and 2b are either both enabled or not, while 5a, 5b and 5c are alternatives. Solid edges indicate control flow, while dotted edges indicate communication.

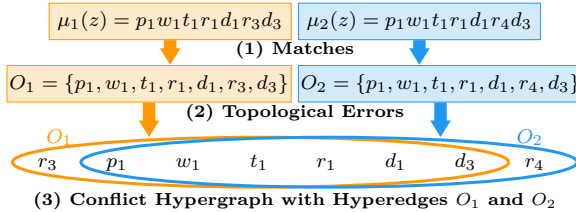


Figure 3: Different encodings of topological errors

minimum among all vertex covers (of \mathcal{H}). Note that, if all vertices have the same weight, minimum weight vertex covers coincide with minimum vertex covers³, which is a stronger notion than that of a minimal vertex cover. Each minimum vertex cover is in turn a minimal vertex cover (but not vice versa). We have the following result, whose proof is available in Appendix B.2.

PROPOSITION 4.7. *Given a minimum weight vertex cover V , removing⁴ all objects in V from G yields a topological repair of G .*

The following integer linear program (ILP) with integer variables x_v , for each vertex $v \in \mathcal{W}$, encodes the problem of finding a minimum weight vertex cover.

$$\begin{aligned} \text{minimize } & \sum_{v \in \mathcal{W}} w(v) \cdot x_v \quad \text{subject to} \quad \sum_{v \in O} x_v \geq 1 \quad \text{for all } O \in \mathcal{E} \\ & \text{and } x_v \in \{0, 1\} \quad \text{for all } v \in \mathcal{W} \end{aligned}$$

Given a solution for this ILP, that is, a function that assigns all variables x_v into $\{0, 1\}$, corresponds to a minimum weight vertex cover V : It consists of all vertices v for which x_v is mapped to 1.

Overall, a repair can be computed by rewriting every constraint into an error query, querying for errors, and then solving the ILP above. Since there are at most exponentially many hyperedges and integer linear programming is in NP, the complete procedure runs in non-deterministic exponential time (data complexity).

Greedy Repairs (Steps 5a and 5b). Despite ILP solvers being reasonably fast in practice, it can be desirable to trade the quality of a repair – in our case, the number of objects deleted – for a better runtime. A common approach to achieve this are so called greedy algorithms, of which we consider two.

³ V is a minimum vertex cover, if there is no vertex cover V' with $|V'| < |V|$.

⁴ Recall that removing a node implies removing all its incident edges in G .

The first we call *naive greedy algorithm*. It computes a vertex cover V_g with a small weight in two phases: the *selection* and the *trimming* phase. In the selection phase the algorithm iterates over all hyperedges to select candidates for the vertex cover: If the current hyperedge contains a vertex, which has already been selected and has minimal weight among the vertices in the hyperedge, the hyperedge is skipped. Otherwise, the algorithm selects an arbitrary vertex from the hyperedge with minimal weight among the vertices in the hyperedge. The selected vertices form a vertex cover V_g , because every hyperedge contains at least one selected vertex.

However, the algorithm may end up selecting too many vertices, and thus V_g might not be *minimal*. Thus, this phase yields an approximate repair. To obtain a repair, the algorithm attempts, in the trimming phase, to reduce the number of selected vertices again. It does this by checking, for every selected vertex v , ordered by weight in descending order, whether there is a hyperedge E for which v is the only selected vertex, i.e. for which $V_g \cap E = \{v\}$ holds. If there is *no* such hyperedge E , then v has to be removed from V_g .

Consider again the two errors $O_1 = \{p_1, w_1, t_1, r_1, d_1, r_3, d_3\}$ and $O_2 = \{p_1, w_1, t_1, r_1, d_1, r_4, d_3\}$. The naive greedy algorithm might compute $V_g = \{r_3, r_4\}$ in the first phase. In the second phase, V_g is not changed, because r_3 and r_4 do not occur in O_2 and O_1 , respectively. Thus, the vertex cover V_g is minimal because neither r_3 nor r_4 can be removed. However, it is not a minimum weight vertex cover, since, e.g., the minimum vertex cover $\{r_1\}$ has a smaller weight.⁵ While the naive greedy algorithm does not necessarily compute a minimum weight vertex cover, picking vertices with minimal weight is sufficient to compute a (topological) repair. Since the algorithm iterates over all errors, it runs in exponential time.

PROPOSITION 4.8. *Given a minimal vertex cover V_g computed by the naive greedy algorithm, removing all objects in V_g from G yields a topological repair of G .*

A proof is available in Appendix B.2.

As for the second greedy algorithm, we consider an *LP-guided greedy algorithm* which combines a solution for the *LP-relaxation* of the ILP with the naive greedy algorithm. Here the LP-relaxation is the linear program (LP) obtained from the ILP by replacing the conditions $x_v \in \{0, 1\}$ with inequalities $0 \leq x_v \leq 1$ and allowing the x_v to assume real values. It is well-known that LPs can be solved

⁵ It is also possible that the naive greedy algorithm picks r_1 instead of r_3 and r_4 in which case it would yield the minimum weight vertex cover $\{r_1\}$.

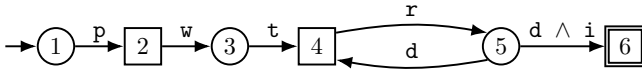


Figure 4: Automaton for the RGPC pattern from Example 3.2

in polynomial time, unlike ILPs. The algorithm then selects any vertex v for which $x_v > 0$ holds as a candidate, and then proceeds as the naive greedy algorithm.

4.3 Optional Step 2: Label Deletions

We continue with the description of optional Step 2 in Figure 2 of our repair pipeline, which allows us to obtain non-topological repairs by deleting labels (in addition to nodes and edges).

Our repair pipeline – whether the ILP or a greedy algorithm is used – deletes nodes only if errors contain isolated nodes (aka paths of length 0). Otherwise, an edge is deleted, since edges have minimal weight 1. This can lead to the presence of (potentially many) isolated nodes in a repair, when all incident edges of a node are deleted. To avoid this case, we study repairs which are not necessarily topological. More precisely, we extend our approach to include the removal of labels to obtain a repair, as discussed in Example 4.1. Instead of deleting (many) incident edges of a node, it can suffice to remove a single label of a node. Note that it is not always possible to obtain a repair by only removing labels, i.e., if a constraint does not refer to any label. Thus, it may still be necessary to delete nodes and/or edges, in addition to deleting labels.

The idea is to extend topological errors O_μ , which initially contain the nodes and edges of the property graph occurring in the co-domain of a match μ , by pairs (o, ℓ) of objects o , i.e. a node or an edge, and labels ℓ . We call these pairs (o, ℓ) *tokens*. The intended meaning is that the error can be repaired by removing the label ℓ from node (or edge) o . The edges of the (not necessarily topological) conflict hypergraph are then all extended sets – which we will simply call *errors* in the following. We note that, in general, there are multiple extensions of a single topological error. In particular, there are more errors than topological errors.

In the following we discuss how to compute errors given a match. We start with the simple case of a single constraint with a single path pattern. Consider once again the constraint from Example 3.2. Recall that it consists of one path pattern with path variable z . We can observe that removing the person label from the node p_1 , or removing the works_on from the edge w_1 yields a repair. Indeed, every path matching the pattern of the constraint has to start with a node labelled person followed by an edge labelled works_on, and p_1 and w_1 are the only objects with these labels. Thus, (p_1, person) is a token we are looking for. The same is true for $(w_1, \text{works_on})$. We say that these tokens are *essential*.

Automata Construction (Step 2a). To compute essential tokens automatically for arbitrary RGPC path patterns, we construct automata, which we call *RGPC automata* and introduce next, by means of an example. Consider the path pattern

$$(x : p) \xrightarrow{w} (u : t) [\xrightarrow{d} (: d)]^+ (y : d \wedge i)$$

from Example 3.2. The RGPC automaton for this path pattern is illustrated in Figure 4. Note that the transitions are labelled with

label expressions, i.e. propositional formula connecting labels – instead of just (single) labels. For instance, the transition from state 5 to 6 is labelled with $d \wedge i$, which is the label expression of the node pattern $(y : d \wedge i)$. Thus, RGPC automata belong to the family of so called *symbolic* automata [see, e.g., 14]. A transition can be taken if the label expression is satisfied by the *set* of labels of a node or edge. For instance, the transition with the formula $d \wedge i$ actually represents several transitions: one for each set of labels that contains d and i . Notably, the transition from State 5 to State 4 can also be taken if d and i are both present. This allows the automaton to read traces of paths, e.g. the trace $\{p\}\{w\}\{t\}\{r\}\{d, i\}\{r\}\{d, i\}$ of the path $p_1 w_1 t_1 r_1 d_1 r_3 d_3$ from the end of Section 2.1.

Furthermore, unlike classical automata, the RGPC automaton illustrated in Figure 4 has two kinds of states: Those drawn as a circle and those drawn as a square, indicating that the next transition reads the label(s) of a node or the label(s) of an edge, respectively. For instance, the outgoing transition of State 1 originates from the node pattern $(: p)$, and the outgoing transition of State 2 from the edge pattern \xrightarrow{w} . In particular, the RGPC automaton reads node and edge labels in alternation, and can thus read the trace of a path.

Finally, note that variables of the path pattern do not play a role for the automaton construction: We use RGPC automata to rescan paths returned during the error retrieval step (Step 1). We thus already know that such a path is a match, and we are only interested in identifying labels for deletions.

The formal RGPC automata construction is available in Appendix B.1.

Algorithm 1: Computing Errors with Essential Tokens for a Single Path

```

Input: Match  $\mu$ , path pattern  $z = \mathcal{P}$ ,  $\mu(z) = v_0 e_1 v_1 \dots e_n v_n$ 
Output: Set of errors  $\mathcal{E}_\mu$  with essential tokens
1  $\mathcal{A} \leftarrow$  automaton for  $\mathcal{P}$ ;
2  $O_\mu \leftarrow \{v_0, e_1, v_1, \dots, e_n, v_n\}$ ; // topological error
3  $\mathcal{E}_\mu \leftarrow \emptyset$ ; // set of errors
4 foreach accepting run  $r$  of  $\mathcal{A}$  on path  $\mu(z)$  do
5    $O_r \leftarrow \emptyset$ ;
6   foreach  $o \in O_\mu$  and label  $\ell$  do
7     if removing  $\ell$  from  $o$  invalidates  $r$  then
8       |  $O_r \leftarrow O_r \cup \{(o, r)\}$ ; //  $(o, \ell)$  is essential
9    $O_{\mu, r} \leftarrow O_\mu \cup O_r$ ;  $\mathcal{E}_\mu \leftarrow \mathcal{E}_\mu \cup \{O_{\mu, r}\}$ ;
10 return  $\mathcal{E}_\mu$ 

```

Computing Essential Tokens (Step 2b). Our algorithm for computing errors for a single path pattern \mathcal{P} is outlined in Algorithm 1. It uses the automata constructed in Step 2a to identify essential tokens, as follows: Let z be the path variable of \mathcal{P} and \mathcal{A} be the automaton constructed for it, and μ be a match of \mathcal{P} . Then \mathcal{A} accepts the trace of the path $\mu(z)$. To obtain essential tokens, we consider every accepting run r of \mathcal{A} on the trace of $\mu(z)$: if removing a label ℓ from an object o on the path $\mu(z)$ invalidates the run, it is *essential for this run*. For example, the trace $\{p\}\{w\}\{t\}\{r\}\{d, i\}\{r\}\{d, i\}$ is accepted by the automaton depicted in Figure 4. Removing the label i from the last set in the trace invalidates all accepting runs, because the automaton can no longer take the transition from state 5 to 6

after reading the second $\{r\}$ (and if the transition is taken earlier the automaton cannot read the whole trace).

For invalidating the match μ , all accepting runs have to be invalidated. Thus, for each accepting run r , we extend O_μ to the error $O_{\mu,r}$ by adding all tokens which are essential for r . Note that, if the pattern does not contain any labels, there are no essential tokens for any run. In that case, the original error O_μ is kept as is.

Suppose now the constraint consists of a graph pattern q with k path patterns, with path variables z_1, \dots, z_k . Let μ be a match witnessing that the constraint is not satisfied. Let further \mathcal{A}_i be the automaton for pattern $i \in \{1, \dots, k\}$, and r_1, \dots, r_k be accepting runs of $\mathcal{A}_1, \dots, \mathcal{A}_k$ on the traces of the paths $\mu(z_1), \dots, \mu(z_k)$. While it suffices to invalidate one of these runs, to invalidate the combination r_1, \dots, r_k , we observe that there might be other combinations involving the same runs: Say we invalidated an accepting run r_j by deleting some label. Then the runs $r_1, \dots, r_j, \dots, r_k$ do no longer witness that μ is a match. However, there might be another run r'_j such that $r_1, \dots, r'_j, \dots, r_k$ still witness that μ is a match.

We thus create an error for every combination r_1, \dots, r_k of accepting runs. More precisely, we condense the sets $O_{\mu,r_1}, \dots, O_{\mu,r_k}$ into a single error $O_{\mu,r_1, \dots, r_k} = O_{\mu,r_1} \cup \dots \cup O_{\mu,r_k}$. The sets O_{μ,r_1, \dots, r_k} , for each match μ and all combinations of runs r_1, \dots, r_k , are then the hyperedges of the *conflict hypergraph*. This way all combinations have to be invalidated by removing (at least) one object.

Since removing a node or edge implies the removal of all its labels, we adapt the weights accordingly: For an edge, the weight is the number of its labels plus 1, and for a node the sum of the number of its labels, the weights of its incident edges, and 1 (for itself). A token (o, ℓ) represents a single label, and thus has weight 1.

We emphasize that Proposition 4.7 does *not* carry over, since the formulas occurring in an RGPC pattern can contain negations: Thus, deleting labels can lead to new matches, and hence, to new errors. We call an RGPC constraint *positive* if *no* label expression in its pattern contains any negation. We then have the following.

PROPOSITION 4.9. *A repair with label removals can be computed in non-deterministic exponential time (data complexity), if the given RGPC constraints are positive.*

4.4 Optional Step 3: Neighbourhood Errors

The optional Step 3 attempts to reduce the runtime by limiting the size of errors, and thus also the number of errors. As a trade-off the repair pipeline yields, in general, an approximate repair.

The size of errors does depend on the size of the considered property graph, and the number of errors can be exponential. We address this problem by introducing neighbourhood errors: In a nutshell, the idea is to repair a property graph by removing objects “close” to the endpoints of the paths inducing errors.

For an integer $k \geq 1$, which can intuitively be understood as a radius around the endpoints of a path, the *k-endpoint neighbourhood* of a path $v_0e_1v_1e_2 \dots e_nv_n$ consists of the objects which have distance at most k from one of the endpoints v_0 and v_n , that is, the objects $v_0, e_1, v_1, \dots, e_k, v_k$ and $v_{n-k}, e_{n+1-k}, v_{n+1-k}, \dots, e_n, v_n$.

Given an RGPC constraint $q; F \Rightarrow C$ with ℓ path variables z_1, \dots, z_ℓ , and a match μ for q witnessing that the constraint is *not* satisfied, the *topological k-neighbourhood error* O_μ^k consists of

all nodes and edges o , for which there is a path variable z_i , $1 \leq i \leq \ell$, such that o occurs in the k -endpoint neighbourhood of $\mu(z_i)$.

When Step 3 is enabled, the pipeline uses (topological) k -neighbourhood errors in place of (topological) errors. For example, consider once more the constraint from Example 3.2, the property graph depicted in Figure 1, and recall that there are two matches witnessing that the property graph does not satisfy the constraint: The first match corresponds to the path $p_1w_1t_1r_1d_1r_3d_3$ (cf. Example 2.3), and the second one to the path $p_1w_1t_1r_1d_1r_4d_3$. The topological 1-neighbourhood errors are $O_1^1 = \{p_1, w_1, t_1\} \cup \{d_1, r_3, d_3\}$, and $O_2^1 = \{p_1, w_1, t_1\} \cup \{d_1, r_4, d_3\}$. In contrast to the (full) topological errors $O_1 = \{p_1, w_1, t_1, r_1, d_1, r_3, d_3\}$ and $O_2 = \{p_1, w_1, t_1, r_1, d_1, r_4, d_3\}$, the edge r_1 is missing from O_1^1 and O_2^1 . Thus, when using O_1^1 and O_2^1 instead of O_1 and O_2 , the repair obtained by deleting r_1 is not found. On the other hand, the errors are smaller, and in general their size is bounded linearly in k , and not in the size of the property graph.

5 EXPERIMENTS

To showcase that our approach is applicable in practice we conducted several experiments: We first assess the base pipeline in terms of runtimes and scalability with respect to the number of errors and constraints, and compare the performances and quality of the ILP and both greedy algorithms. We then study the effects of the optional steps of the repair pipeline on quality and runtime. Finally, we conduct a qualitative study aiming at studying the behaviour of the pipeline on a real-world dataset with real-world constraints. For the evaluation, we use the four property graphs of different sizes listed in Table 1. The top three are real-world property graphs, and the LDBC property graph is generated with the corresponding benchmark. We implemented our repair pipeline [41], illustrated in Figure 2, in Python 3.13. For solving (I)LPs, we use HiGHS [28]. As graph database system, we use Neo4j 5.26 (community edition). All experiments were run on a virtual machine with 8 physical cores of an Intel(R) Xeon(R) Silver 4214 CPU [17] and 125GiB RAM.

5.1 Assessing the Base Pipeline

In this section, we assess the performance and quality of the *base pipeline*, that is our repair pipeline without any optional steps. For this purpose, we generated constraints with pattern shapes as outlined in Figure 5 for the property graphs in Table 1. These pattern shapes cover most shapes that have been observed in real-life query logs [9] while also exhibiting recursion. Notably, the 1-way shape alone covers 74.61% of the valid path patterns observed [9], and the loop shapes include triangles, since the orange dashed shape can take the form of a pattern which matches paths of length 2. An instance of a 1-way pattern with 3 edge and 4 node patterns is $z = [(:a) \xrightarrow{c} (:b) \xrightarrow{e} (:d) \xrightarrow{f} (:h)]^+$. A constraint then consists of a pattern combined with an empty filter and the condition `{false}`. This maximizes the number of errors for our scaling experiments. Moreover, to increase the number of constraints (and errors), we added, to each graph, an additional 10% of edges – labelled with a special label – randomly between nodes, which were already connected by an edge in the original graph, to preserve the topology. We emphasize that there is no correlation between the additional edges and errors: they can partake in an error or not, like other edges. Their sole purpose is to *increase* the number of paths, and

Table 1: Property graphs used for experiments, number $|\Sigma|$ of constraints, and number of errors

Name	#Nodes	#Edges	1-way		2-rep		2-way		loop		3-split	
			$ \Sigma $	#errors								
ICIJ Property Graph [29]	2 016 523	3 339 267	14	558799	19	397108	39	7553	188	56614	152	876933
Italian Legislative Graph [15, 16]	411 787	1 117 528	20	166977	—	—	53	443695	61	3783	—	—
Coreutils Code Property Graph [45]	206 506	387 284	20	45728	—	—	52	3707	—	—	—	—
LDBC, scaling factor 0.3 [1, 2]	940 322	5 003 201	5	79064	6	72756	—	—	56	423	4	2734499

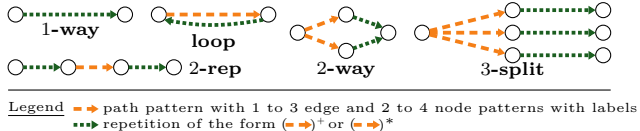


Figure 5: Shapes of RGPC patterns used in Sections 5.1 and 5.3

hence errors. The number of constraints and the total number of errors, for each shape and property graph, are listed in Table 1. Note that no ground truth is available. Instead, the given graphs are regarded as dirty, and our repairs are clean by definition. The repairs obtained by the ILP algorithm serve as best possible repairs.

We compare the performance and quality of the two greedy and ILP algorithms. We use runtimes⁶ as performance, and the number of deletions as quality measure – a smaller number of deletions means a higher quality since it corresponds to less information loss. Note that measures like the F_1 -score for quality are not meaningful: since our holistic approach always repairs all errors, there are no false negatives, and by definition a repair cannot contain false positives. Hence, the F_1 -score is always 1 (or 0 in case of a timeout).

Figures 6a to 6d show the runtime of the naive greedy (NG), LP-guided greedy (LPG), and the ILP algorithms. Note that we used a log-scaled y-axis to obtain readable plots. For example, Figure 6a shows the performance of the base pipeline when run on the legislative property graph with the sets of 1-way, 2-way, and loop constraints outlined in Table 1. The ILP algorithm takes in general more time than the naive greedy algorithm, and as a trade-off, it deletes less objects⁷, cf. Figures 7a to 7d (which also have a log-scaled y-axis, but a different range than the runtime plots). The LP-guided greedy achieves the same quality as the ILP algorithm in almost all cases (cf. Figures 7a to 7d). At the same time it competes with the naive greedy algorithm performance-wise. In many cases it even performs better. Inspecting the solutions of the LP-solver revealed that it converges towards integral solutions in these cases.

Overall, the experiments show that the LP-guided greedy algorithm yields higher-quality repairs with about 35% fewer deletions than the naive greedy, matching the quality of repairs yielded by the ILP algorithm. It also offers a runtime advantage of over 97% (Figure 6c, 2-way) compared to the ILP strategy, and beats the naive greedy algorithm in a case where the ILP one timed out (Figure 6d, 1-way). These observations in the general case are however not

always true as demonstrated by Figure 6c (ICIJ): the ILP algorithm outperforms both greedy algorithms for 1-way constraints, which exhibit a high number of errors with paths containing many cycles.

Approximate Repairs. We now investigate approximate repairs and deepen the comparison between the naive and the LP-guided greedy algorithms by disabling the trimming phase in the pipeline. The results for the ICIJ graph are shown in Figures 6e and 7e. We observe that the selection phase of the naive greedy performs better than the one of the LP-guided greedy, and compared with the full runtimes in Figure 6c, the trimming phase is responsible for the majority of the runtime for both. In particular, the trimming phase of the naive greedy is responsible for making it perform worse overall. Correlating the number of proposed edge deletions indicates that this is because, for the naive greedy, more edge deletions are trimmed. When comparatively many edge deletions have to be trimmed for the LP-guided greedy, it can be outperformed by the naive greedy algorithm (e.g. ICIJ, 2-rep). Lastly, the selection phase of the LP-guided greedy algorithm can yield a good approximation or even a proper repair in the majority of cases, with a 89% reduction in runtime (1-way). Similar results for the other datasets are provided in Appendix C.

Scalability. As for the scalability of our pipeline with respect to the numbers of constraints and errors, Figures 6c and 6a attest that our pipeline can handle up to 188 loop constraints for the ICIJ graph, while it runs into a timeout for the smaller legislative graph with 53 2-way constraints. Regarding the size of errors, the maximal size we observed were 73 objects (Legislative, loop). Figure 6d shows that over 2.7 million errors due to 3-split constraint can be repaired comparatively fast, while 79064 errors due to 1-way constraints are challenging. Comparing the results for 1-way constraints for the ICIJ and LDBC graphs, we observe that our pipeline performs better for the former, even though there are fewer constraints (of the same shape) and fewer errors for the smaller LDBC graph (cf. Table 1, 1-way column). To investigate this case further, we ran the experiments for the ICIJ and LDBC graphs with subsets of 1-way constraints, and thus fewer errors. The resulting runtimes are shown in Figures 8a and 8b, and the number of deletions in Figures 8c and 8d. The y-axes in these plots are labelled with the numbers of errors. For the LDBC graph, compared to the number of errors, a high number of edges are deleted – up to 67% for the LP-guided greedy and ILP algorithms, and 73% for naive greedy algorithm – while only very few deletions are necessary to repair the ICIJ graph. This indicates that our repair pipeline performs well, if the repair can be achieved with a low number of deletions. Constraints and number of errors play a relatively negligible role.

⁶We do not measure error detection via queries, which heavily depends on the database system and is not the focus of our paper.

⁷Due to the nature of our constraints, the pipeline always opts for deleting edges without any optional feature enabled.

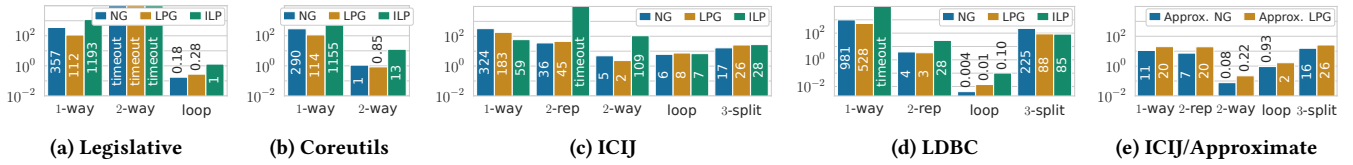


Figure 6: Runtimes in seconds of the naive greedy (NG), LP-guided greedy (LPG), and the ILP algorithms

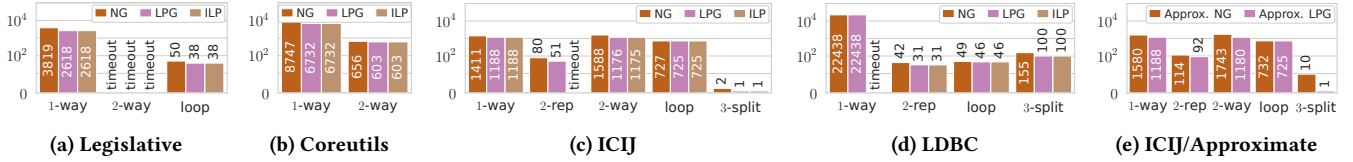


Figure 7: Number of edge deletions proposed by the naive greedy (NG), LP-guided greedy (LPG), and the ILP algorithms

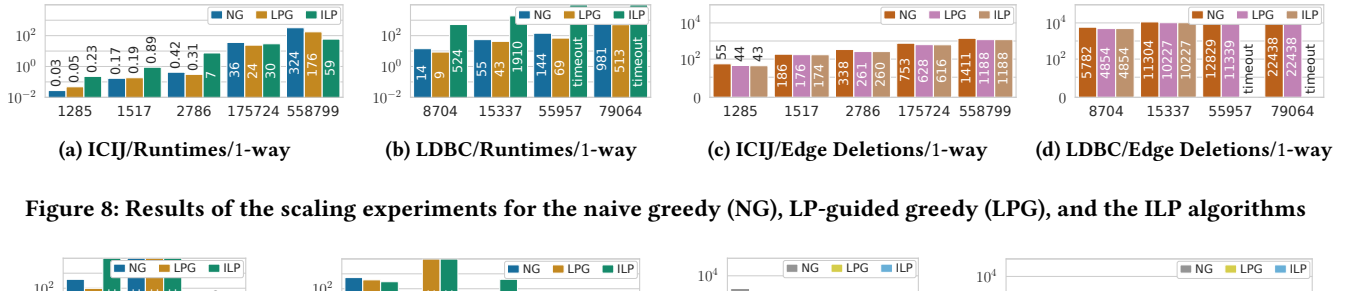


Figure 8: Results of the scaling experiments for the naive greedy (NG), LP-guided greedy (LPG), and the ILP algorithms

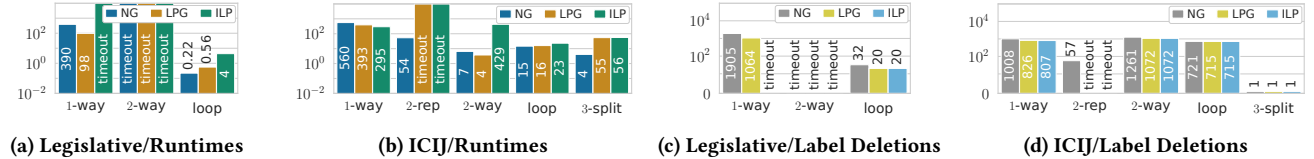


Figure 9: Runtimes (in seconds) with Step 2 enabled and number of label deletions for the legislative and ICIJ graphs

5.2 Minimizing Deletions of Important Objects

By default our pipeline assigns uniform weights to edges, and node weights are determined by degree. To improve robustness, we allow the pipeline to incorporate varying *custom weights* $w_c(o) > 0$ for nodes and edges $o \in N \cup E$, stored as property values in the property graph, with the aim of reducing the deletion of objects deemed “important”. Internally, the weight $w_c(e)$ of an edge is then $w_c(e)$, and the weight $w_c(n)$ of a node is $w_c(n)$ plus the sum of all $w_c(e)$, for all incident edges e . The objective of the pipeline is then shifted from minimizing the number of deletions to minimizing the reduction of the total custom weight across all nodes and edges.

To assess this feature, we used PageRank scores as weights for nodes and edges⁸. Without custom weights, the total PageRank value decreases by 0.09% (1-way constraints) when applying the LP-guided greedy algorithm on the ICIJ graph. With custom weights, the decrease is limited to 0.07% (2-way constraints), corresponding to a 24% reduction in weight loss, indicating that fewer high-weight edges are deleted. The number of deletions is shown in Figure 10d, and compared with Figure 7c, showing an increase ranging from

⁸Page rank for edges are computed using the line graph: Every edge becomes a node, and there is an edge (e_1, e_2) if there is a path $v_0e_1v_1e_2v_2$ in the original graph.

1% (2-rep constraints) to 43% (2-way constraints). The runtimes are shown in Figure 10c. Compared with the base case in Figure 6c, custom weights can have a positive or negative impact on runtime. More details are provided in Appendix C.

5.3 Label Removals and Neighbourhood Repairs

We now evaluate the optional steps of our pipeline, and compare them to the base pipeline established in Section 5.1.

To show the effects of Step 2, we present the runtimes and number of label deletions for the legislative and the ICIJ graph in Figure 9. Recall that extending errors with essential tokens results in more, and larger errors. Consequently, the (I)LPs are also larger. Furthermore, there tend to be more equally weighted repairs: instead of deleting an edge, there is now the choice between deleting any label from the edge, or one of its endpoints. The runtimes increase considerably – by up to 500% (Figure 6c vs. Figure 9b, 1-way). The ILP algorithm even timed out in one more case (Figure 9a, 1-way).

However, comparing with Figures 7a and 7c, we observe a reduction of up to 50% of object deletions for the naive greedy algorithm (Legislative, 1-way), of up to 47% for the ILP algorithm (Legislative, loop), and of up to 59% for the LP-guided greedy (Legislative, 1-way, the ILP algorithm times out in this case, cf. Figure 9c).

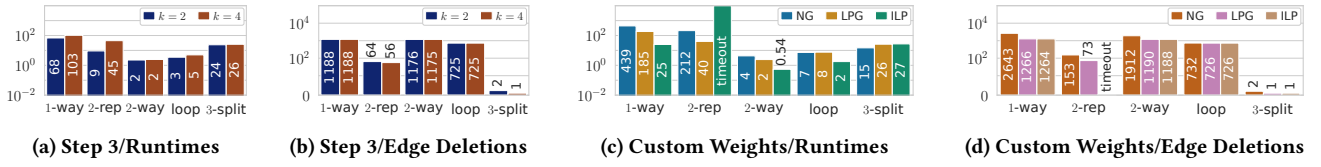


Figure 10: Results of the LP-guided greedy algorithm for neighbourhood (Step 3) and custom weight repairs for ICIJ

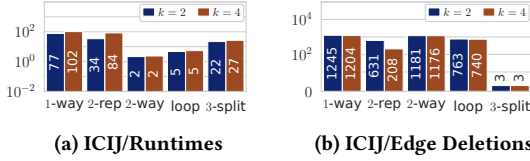


Figure 11: LP-guided greedy algorithm on sampled errors

Notably, even the naive greedy algorithms can yield a repair with less label deletions than the ILP with (only) edge deletions (Legislative, 1-way). Note that the greedy algorithms can sometimes even be faster if label deletions are allowed which has to be attributed to the structure of the errors and the (I)LP (e.g. Figure 9a, 1-way).

A similar trend can be observed for the other datasets; for space reasons they are provided in Appendix C.

With Step 3 we observe a runtime reduction of up to 62% compared to the base pipeline while maintaining almost the same quality, i.e. number of deletions. We present the runtimes and number of proposed edge deletions for ICIJ and neighbourhood $k = 2$ as well as $k = 4$ in Figures 10a and 10b, for the LP-guided greedy algorithm. Compared to the base case shown in Figure 6c, the performance is better in cases where the base pipeline takes a significant amount of time, i.e. more than a few seconds.

The numbers of deletions are quite similar for $k = 2$ and $k = 4$, and more importantly, the results for the base pipeline as in Figure 7c, except for the experiment for 2-rep constraints. That is, in all cases where matches consisting of *shortest paths* are (almost) completely covered by the k -endpoint neighbourhood.

To assess whether picking the neighbourhoods of path endpoints is a suitable strategy for reducing the size of errors, we performed the same experiments with random samples of errors: that is, we sampled $2k$ edges (and their endpoints) from each error. The result for the LP-guided greedy algorithm on the ICIJ graph is shown in Figure 11. Compared with the result for neighbourhood errors shown in Figure 10, the runtimes do not differ significantly, but the number of deletions can explode if paths are long (9.86x for 2-rep). This suggests that intersections of (topological) errors are indeed more likely to happen near path endpoints, and taking a random sample from a long path is less likely to contain these intersections.

Similar plots to the ones for Steps 2 and 3 for the other datasets are available in Appendix C.

5.4 A Qualitative Study

To showcase that our repair pipeline is viable in practice, we conducted a qualitative study on the real-world ICIJ property graph, which is built and used by the International Consortium of Investigative Journalists. Since this property graph was assembled from

several data sources, it contains some real-world inconsistencies, detected using the RGPC constraints in Table 2.

The constraints are concerned with *entities*, which model companies and organisations, and *officers*, which are persons involved with entities. We note that entities can also be in an *officer_of* relationship with other entities, although neither of them is labelled as an officer. Constraint γ_1 states that entities and/or officers in a *same_name_as* relationship, have indeed the same name. Constraint γ_2 is a typical denial constraint forbidding an entity from having an inactivation date, if it is still active. Constraint γ_3 models an *exclusivity* condition for entities [4]: no entity can have two *sole* directors. Finally, γ_4 ensures that a president of an entity cannot gain an advantage by indirectly influencing another entity they are associated with, through their presidency. The number of errors for each constraint is given in Column 3 of Table 2.

We first discuss the repairs yielded by the base pipeline with the ILP algorithm. The numbers of deletions are given in Column 4 of Table 2. For γ_1 , *same_name_as* relationships are deleted. This preserves the original names stored in the properties (unifying names could lead to false accusations in this scenario). Since errors for this constraint cannot share edges, one deletion per error is expected. Constraint γ_2 is an example where the pipeline is forced to delete nodes, since each error consists of exactly one node. Thus, the nodes are deleted, and consequently so are all their 177 incident edges. For γ_3 one of the two relationships in each error is deleted, which shows that symmetries are resolved properly (the errors do not share any objects in this case). The repair for γ_4 shows that the number of deletions can be significantly less than the number of errors – our pipeline exploits that errors have edges in common.

We investigate robustness w.r.t. graph topology changes with γ_4 , since it encompasses a non-trivial path pattern. Assuming that sub-patterns describing paths of *same_name_as*- and *president_of*-labelled edges are important, we double the weight of these edges. The repair pipeline then proposes the deletion of 14 instead of 10 edges but preserves all of the aforementioned edges. It also preserves at least 168 of 203 matches of the first pattern of γ_4 . Without the custom weights, it preserves only between 96 and 117 matches of this pattern.

When enabling label deletions, the graph can be repaired with 6323 label deletions, which is only about 35% of the 18255 node and edge deletions without it. 1394 labels are removed from edges, effectively deleting the concrete relationship but preserving the knowledge that there is some (potential) relationship.

Using the naive greedy algorithm instead of the ILP algorithm resulted in up to 2 more deletions for γ_4 (depending on the order in which the database returned errors), the same amount of deletions for the other constraints. The LP-guided greedy yielded the same number of deletions. With the ILP algorithm taking under 4 seconds

Table 2: Real-world like RGPC constraints for the ICIJ property graph

ID	RGPC constraint $q; F \Rightarrow C$	#errors	#deletions
γ_1	$(x:Entity \vee Officer) \xrightarrow{\text{:same_name_as}} (y:Entity \vee Officer); \emptyset \Rightarrow \{x.name = y.name\}$ $\hookrightarrow \text{All entities and officers in a same_name_as relationship have indeed the same name.}$	18000	18000 edges 0 nodes
γ_2	$(x:Entity); \{x.inactivation_date \leq 2025-07-01\} \Rightarrow \{x.status \neq \text{"Active"}\}$ $\hookrightarrow \text{All entities with an inactivation date in the past do not have the status "Active".}$	46	177 edges 46 nodes
γ_3	$(x:Officer) \xrightarrow{\text{:sole_director_of}} (y:Entity), (z:Officer) \xrightarrow{\text{:sole_director_of}} (y); \emptyset \Rightarrow \{x = z\}$ $\hookrightarrow \text{An entity cannot have more than one sole director.}$	44	22 edges 0 nodes
γ_4	$(x:Officer) \xrightarrow{\text{:president_of}} (y:Entity)[(:Entity \vee Officer) \xrightarrow{\text{:officer_of \vee same_name_as}}]^+ (z:Entity), (x) \xrightarrow{\text{:officer_of}} (z); \emptyset \Rightarrow \{y = z\}$ $\hookrightarrow \text{No president is indirectly in control of an entity, e.g. through a chain of shell companies, they are directly an officer of.}$	19	10 edges 0 nodes

for the set of all constraints, there is no advantage of using either greedy algorithm or neighbourhood errors in this scenario.

6 RELATED WORK

Error repairing for PG-Constraints has not been addressed in prior work besides the assessment that PG-Constraints can be rewritten into GQL queries for querying errors [4].

Error repairing for less expressive graph data models, such as labelled graphs, focuses on chase-based approaches [10, 11, 21, 22, 32, 38, 39], which iteratively add properties, or even edges to repair a graph. Thus, this repair mode is orthogonal to our delete-based approach, and consequently not comparable. In particular, insertion-only repair modes are not suitable for repairing violations of denial constraints in our examples and experimental settings [20].

A different approach for repairing graphs is with respect to neighbourhood constraints, that is, constraints which restrict the labels of a node depending on the labels of its neighbours [40]. Their repair mode involves changing labels, and, if that is not enough, changing the neighbourhood of a node, which is again incompatible with our repair mode. They introduce a greedy variant of their algorithm to strike a balance between runtime and repair quality.

User-centric repairs for property graphs have been studied [36], albeit w.r.t. constraints for less expressive graph data models. Their repair model focuses on label and property changes, but also allows the deletion of edges as fall-back. Letting users repair errors consisting of variable-length paths requires carefully crafted human-machine interfaces, which is beyond the scope of this work.

The idea of using vertex covers of conflict hypergraphs originates from theoretical work for repairing relational databases [12, 42], but these repairs do not involve dependencies between objects and arbitrary long paths. A notable consequence is that, unlike in the relation setting, not every minimal vertex cover corresponds to a repair, which we addressed by using minimum weighted vertex covers. We note that modelling dependencies explicitly (like foreign-key constraints) instead of using weights, yields an unreasonable amount of (artificial) errors in the case of property graphs, since they would involve all nodes, edges, and labels. For the vast literature on error repairing for other database models and repair modes, including the relational model, we refer to surveys [13, 19].

We note that the vertex cover problem for hypergraphs is even W[2]-hard [25], which means that it is very unlikely that there is an FPT algorithm. A common strategy for solving ILPs are LP-rounding algorithms [e.g., 35], which solve the LP variant of the ILP and then

use *randomized rounding* to obtain an integral solution. Our LP-guided greedy algorithm uses a trivial rounding step instead, which is arguably sufficient, as shown by our experiments in Section 5.

Theoretical foundations for RGPC patterns have been investigated, in particular CRPQs with path variables [6, 23], which even allow for “regular” comparisons of paths. Notably, unlike RGPC patterns, CRPQs only match edge labels (i.e. no node labels), and do not support label expressions. The same differences apply to our RGPC automata model and automata constructed for CRPQs [6].

Lastly, we defined RGPC patterns as a syntactical fragment of GPC patterns to abstract core features of the pattern matching sub-language of GQL and SQL/PGQ [26]. A useful feature in practice and supported by these languages are patterns which allow for traversing edges in reverse direction. We outline how our pipeline can be extended with this feature and other differences in Appendix A.3. It is known that enumerating matches of GPC patterns is in polynomial space in the size of the property graph but not in polynomial space in the size of the pattern [26]; making the enumeration of all errors in large graphs intractable, and sets boundaries for repair procedures relying on enumerating all errors. Finally, PG-Constraints can capture dependencies based on regular path queries for which problems related to graph repair like certain query answering are undecidable [see, e.g. 7, 27, 37].

7 CONCLUSION AND FUTURE WORK

In this paper, we addressed error repairing for property graphs under PG-Constraints. We designed a repair pipeline for RGPC constraints with user-selectable trade-offs and demonstrated its effectiveness through extensive experiments.

As future work, we plan to study the practical limits of error repairing under PG-Constraints. Additional features could be incorporated such as advanced GQL pattern matching [18, 24]. The repair model may also be extended to allow property deletions, though this is challenging since deletions can introduce new errors. Other repair modes could combine our deletion-based approach with insertion techniques from the state of the art. Finally, given the large number of errors recursive constraints may generate, and inspired by work on incremental error detection in the relational setting [31], we aim to explore how errors can be efficiently prevented from being inserted in the first place.

ACKNOWLEDGMENTS

The authors were supported by ANR-21-CE48-0015 VeriGraph. A. Bonifati is also funded by IUF Endowed Chair.

REFERENCES

[1] Renzo Angles, János Benjamin Antal, Alex Averbuch, Peter Boncz, Orri Erling, Andrey Gubichev, Vlad Haprian, Moritz Kaufmann, Josep Lluís Larriba-Pey, Norbert Martínez-Bazán, József Marton, Marcus Paradies, Minh-Duc Pham, Arnau Prat-Pérez, Mirko Spasic, Benjamin A. Steer, Gábor Szárnýas, and Jack Waudby. 2020. The LDBC Social Network Benchmark. <https://doi.org/10.48550/arxiv.2001.02299> arXiv:2001.02299

[2] Renzo Angles, Peter A. Boncz, Josep Lluís Larriba-Pey, Irini Fundulaki, Thomas Neumann, Orri Erling, Peter Neubauer, Norbert Martínez-Bazán, Venelin Kotsev, and Ioan Toma. 2014. The linked data benchmark council: a graph and RDF industry benchmarking effort. *ACM SIGMOD Record* 43, 1 (May 2014), 27–31. <https://doi.org/10.1145/2627692.2627697>

[3] Renzo Angles, Angela Bonifati, Stefania Dumbrava, George Fletcher, Alastair Green, Jan Hidders, Bei Li, Leonid Libkin, Victor Marsault, Wim Martens, Filip Murlak, Stefan Plantikow, Ognjen Savkovic, Michael Schmidt, Juan Sequeda, Slawek Staworko, Dominik Tomaszuk, Hannes Voigt, Domagoj Vrgoc, Mingxi Wu, and Dusan Zivkovic. 2023. PG-Schema: Schemas for Property Graphs. *Proceedings of the ACM on Management of Data* 1, 2 (June 2023), 1–25. <https://doi.org/10.1145/3589778>

[4] Renzo Angles, Angela Bonifati, Stefania Dumbrava, George Fletcher, Keith W. Hare, Jan Hidders, Victor E. Lee, Bei Li, Leonid Libkin, Wim Martens, Filip Murlak, Josh Perryman, Ognjen Savkovic, Michael Schmidt, Juan F. Sequeda, Slawek Staworko, and Dominik Tomaszuk. 2021. PG-Keys: Keys for Property Graphs. In *SIGMOD '21: International Conference on Management of Data, Virtual Event, China, June 20–25, 2021*, Guoliang Li, Zhanhuai Li, Stratos Idreos, and Divesh Srivastava (Eds.). ACM, New York, NY, USA, 2423–2436. <https://doi.org/10.1145/3448016.3457561>

[5] Marcelo Arenas, Leopoldo E. Bertossi, and Jan Chomicki. 1999. Consistent Query Answers in Inconsistent Databases. In *Proceedings of the Eighteenth ACM SIGACT-SIGMOD-SIGART Symposium on Principles of Database Systems, May 31 - June 2, 1999, Philadelphia, Pennsylvania, USA (SIGMOD/PODS99)*, Victor Vianu and Christos H. Papadimitriou (Eds.). Association for Computing Machinery (ACM) Press, New York, NY, USA, 68–79. <https://doi.org/10.1145/303976.303983>

[6] Pablo Barceló, Leonid Libkin, Anthony W. Lin, and Peter T. Wood. 2012. Expressive Languages for Path Queries over Graph-Structured Data. *ACM Transactions on Database Systems* 37, 4 (Dec. 2012), 1–46. <https://doi.org/10.1145/2389241.2389250>

[7] Catriel Beeri and Moshe Y. Vardi. 1981. The Implication Problem for Data Dependencies. In *Automata, Languages and Programming, 8th Colloquium, Acre (Akko), Israel, July 13–17, 1981, Proceedings* (1981) (Lecture Notes in Computer Science), Shimon Even and Oded Kariv (Eds.), Vol. 115. Springer Berlin Heidelberg, Berlin, Heidelberg, 73–85. https://doi.org/10.1007/3-540-10843-2_7

[8] Philip Bohannon, Michael Flaster, Wenfei Fan, and Rajeev Rastogi. 2005. A Cost-Based Model and Effective Heuristic for Repairing Constraints by Value Modification. In *Proceedings of the ACM SIGMOD International Conference on Management of Data, Baltimore, Maryland, USA, June 14–16, 2005 (SIGMOD/PODS05)*, Fatma Özcan (Ed.). Association for Computing Machinery (ACM), New York, NY, USA, 143–154. <https://doi.org/10.1145/1066157.1066175>

[9] Angela Bonifati, Wim Martens, and Thomas Timm. 2020. An Analytical Study of Large SPARQL Query Logs. *The VLDB Journal* 29, 2–3 (May 2020), 655–679. <https://doi.org/10.1007/s00778-019-00558-9>

[10] Yurong Cheng, Lei Chen, Ye Yuan, and Guoren Wang. 2018. Rule-Based Graph Repairing: Semantic and Efficient Repairing Methods. In *34th IEEE International Conference on Data Engineering, ICDE 2018, Paris, France, April 16–19, 2018*. IEEE Computer Society, 773–784. <https://doi.org/10.1109/ICDE.2018.000075>

[11] Yurong Cheng, Lei Chen, Ye Yuan, Guoren Wang, Boyang Li, and Fusheng Jin. 2022. Strict and Flexible Rule-Based Graph Repairing. *IEEE Transactions on Knowledge and Data Engineering* 34, 7 (2022), 3521–3535. <https://doi.org/10.1109/TKDE.2020.3019817>

[12] Jan Chomicki and Jerzy Marcinkowski. 2005. Minimal-Change Integrity Maintenance Using Tuple Deletions. *Information and Computation* 197, 1–2 (Feb. 2005), 90–121. <https://doi.org/10.1016/J.IC.2004.04.007>

[13] Xu Chu, Ihab F. Ilyas, Sanjay Krishnan, and Jiannan Wang. 2016. Data Cleaning: Overview and Emerging Challenges. In *Proceedings of the 2016 International Conference on Management of Data (2016-06) (SIGMOD/PODS'16)*. Association for Computing Machinery (ACM), San Francisco California USA, 2201–2206. <https://doi.org/10.1145/2882903.2912574>

[14] Alessandro Cimatti, Sergio Mover, Marco Roveri, and Stefano Tonetta. 2011. From Sequential Extended Regular Expressions to NFA with Symbolic Labels. In *Implementation and Application of Automata*, Michael Domaratzki and Kai Salomaa (Eds.). Vol. 6482. Springer Berlin Heidelberg, Berlin, Heidelberg, 87–94. https://doi.org/10.1007/978-3-642-18098-9_10

[15] Andrea Colombo, Anna Bernasconi, and Stefano Ceri. 2024. *Italian Legislative Property Graph*. Zenodo. <https://doi.org/10.5281/zenodo.11210265>

[16] Andrea Colombo, Anna Bernasconi, and Stefano Ceri. 2024. Modelling Legislative Systems into Property Graphs to Enable Advanced Pattern Detection. <https://doi.org/10.48550/ARXIV.2406.14935> arXiv:2406.14935

[17] Intel Corporation. 2026. Specification of the Intel(R) Xeon(R) Silver 4214 Processor. <https://www.intel.com/content/www/us/en/products/sku/193385/intel-xeon-silver-4214-processor-16-5m-cache-2-20-ghz/specifications.html>. Accessed: 2026-01-26.

[18] Alin Deutsch, Nadime Francis, Alastair Green, Keith Hare, Bei Li, Leonid Libkin, Tobias Lindaaker, Victor Marsault, Wim Martens, Jan Michels, Filip Murlak, Stefan Plantikow, Petra Selmer, Oskar Van Rest, Hannes Voigt, Domagoj Vrgoč, Mingxi Wu, and Fred Zemke. 2022. Graph Pattern Matching in GQL and SQL/PGQ. In *Proceedings of the 2022 International Conference on Management of Data (2022-06) (SIGMOD/PODS '22)*. Association for Computing Machinery (ACM), Philadelphia PA USA, 2246–2258. <https://doi.org/10.1145/3514221.3526057>

[19] Ahmed K. Elmagarmid, Panagiotis G. Ipeirotis, and Vassilios S. Verykios. 2007. Duplicate Record Detection: A Survey. *IEEE Transactions on Knowledge and Data Engineering* 19, 1 (Jan. 2007), 1–16. <https://doi.org/10.1109/TKDE.2007.250581>

[20] Wenfei Fan. 2008. Dependencies Revisited for Improving Data Quality. In *Proceedings of the Twenty-Seventh ACM SIGMOD-SIGACT-SIGART Symposium on Principles of Database Systems, PODS 2008, June 9–11, 2008, Vancouver, BC, Canada (SIGMOD/PODS '08)*, Maurizio Lenzerini and Domenico Lembo (Eds.). Association for Computing Machinery (ACM), New York, NY, USA, 159–170. <https://doi.org/10.1145/1376916.1376940>

[21] Wenfei Fan, Wenzhi Fu, Ruochun Jin, Muyang Liu, Ping Lu, and Chao Tian. 2023. Making It Tractable to Catch Duplicates and Conflicts in Graphs. *Proceedings of the ACM on Management of Data* 1, 1 (May 2023), 1–28. <https://doi.org/10.1145/3588940>

[22] Wenfei Fan, Ping Lu, Chao Tian, and Jingren Zhou. 2019. Deducing Certain Fixes to Graphs. *Proceedings of the VLDB Endowment* 12, 7 (March 2019), 752–765. <https://doi.org/10.14778/3317315.3317318>

[23] Diego Figueira and Varun Ramanathan. 2022. When is the Evaluation of Extended CRPQ Tractable?. In *PODS '22: International Conference on Management of Data, Philadelphia, PA, USA, June 12 - 17, 2022 (SIGMOD/PODS '22)*, Leonid Libkin and Pablo Barceló (Eds.). Association for Computing Machinery, New York, NY, USA, 203–212. <https://doi.org/10.1145/3517804.3524167>

[24] Diego Figueira and Miguel Romero. 2023. Conjunctive Regular Path Queries under Injective Semantics. In *Proceedings of the 42nd ACM SIGMOD-SIGACT-SIGAI Symposium on Principles of Database Systems (2023-06) (SIGMOD/PODS '23)*. Association for Computing Machinery (ACM), Seattle WA USA, 231–240. <https://doi.org/10.1145/3584372.3588664>

[25] Jörg Flum and Martin Grohe. 2006. *Parameterized Complexity Theory*. Springer Berlin Heidelberg, Berlin, Heidelberg. <https://doi.org/10.1007/3-540-29953-X>

[26] Nadime Francis, Amélie Gheerbrant, Paolo Guagliardo, Leonid Libkin, Victor Marsault, Wim Martens, Filip Murlak, Liat Peterfreund, Alexandra Rogova, and Domagoj Vrgoc. 2023. GPC: A Pattern Calculus for Property Graphs. In *Proceedings of the 42nd ACM SIGMOD-SIGACT-SIGAI Symposium on Principles of Database Systems (2023-06) (SIGMOD/PODS '23)*. Association for Computing Machinery (ACM), Seattle WA USA, 241–250. <https://doi.org/10.1145/3584372.3588662>

[27] Nadime Francis and Leonid Libkin. 2017. Schema Mappings for Data Graphs. In *Proceedings of the 36th ACM SIGMOD-SIGACT-SIGAI Symposium on Principles of Database Systems (2017-05) (SIGMOD/PODS'17)*. Association for Computing Machinery (ACM), Chicago Illinois USA, 389–401. <https://doi.org/10.1145/3034786.3056113>

[28] Qi Huangfu and J. A. J. Hall. 2018. Parallelizing the Dual Revised Simplex Method. *Mathematical Programming Computation* 10, 1 (Dec. 2018), 119–142. <https://doi.org/10.1007/S12532-017-0130-5>

[29] International Consortium of Investigative Journalists. 2026. ICJ Offshore Leaks Database. <https://offshoreleaks.icij.org/pages/database>. Accessed: 2026-01-26.

[30] ISO Central Secretary. 2024. *Information Technology – Database Languages – GQL (1 ed.)*. Standard ISO/IEC 39075:2024. International Organization for Standardization, Geneva, CH.

[31] Youri Kaminsky, Eduardo H. M. Pena, and Felix Naumann. 2024. Incremental Detection of Denial Constraint Violations. *Proceedings of the VLDB Endowment* 18, 4 (Dec. 2024), 1000–1012. <https://doi.org/10.14778/3717755.3717761>

[32] Selasi Kwashie, Lin Liu, Jixue Liu, Markus Stumptner, Jiuyong Li, and Lujing Yang. 2019. Certus: An Effective Entity Resolution Approach with Graph Differential Dependencies (GDDs). *Proceedings of the VLDB Endowment* 12, 6 (Feb. 2019), 653–666. <https://doi.org/10.14778/3311880.3311883>

[33] Yuxi Liu, Fangzhu Shen, Kushagra Ghosh, Amir Gilad, Benny Kimelfeld, and Sudeepa Roy. 2024. The Cost of Representation by Subset Repairs. *Proceedings of the VLDB Endowment* 18, 2 (Oct. 2024), 475–487. <https://doi.org/10.14778/3705829.3705860>

[34] Andrei Lapatenko and Leopoldo E. Bertossi. 2007. Complexity of Consistent Query Answering in Databases Under Cardinality-Based and Incremental Repair Semantics. In *Database Theory - ICDT 2007, 11th International Conference, Barcelona, Spain, January 10–12, 2007, Proceedings (2006) (Lecture Notes in Computer Science)*, Thomas Schwentick and Dan Suciu (Eds.), Vol. 4353. Springer Berlin Heidelberg, Berlin, Heidelberg, 179–193. https://doi.org/10.1007/11965893_13

[35] Mourad El Ouali, Helena Fohlin, and Anand Srivastav. 2014. A randomised approximation algorithm for the hitting set problem. *Theoretical Computer Science* 555 (Oct. 2014), 23–34. <https://doi.org/10.1016/J.TCS.2014.03.029>

[36] Amedeo Pachera, Angela Bonifati, and Andrea Mauri. 2025. User-Centric Property Graph Repairs. *Proceedings of the ACM on Management of Data* 3, 1 (Feb. 2025), 85:1–85:27. <https://doi.org/10.1145/3709735>

[37] Sylvain Salvati and Sophie Tison. 2024. Containment of Regular Path Queries Under Path Constraints, In 27th International Conference on Database Theory, ICDT 2024, Paestum, Italy, March 25–28, 2024 (2024), Graham Cormode and Michael Shekelyan (Eds.). LIPICS, Volume 290, ICDT 2024 290, 17:1–17:19. <https://doi.org/10.4230/LIPICS.ICDT.2024.17>

[38] Larissa Capobianco Shimomura, George Fletcher, and Nikolay Yakovets. 2020. GGDs: Graph Generating Dependencies. In *CIKM '20: The 29th ACM International Conference on Information and Knowledge Management, Virtual Event, Ireland, October 19–23, 2020 (CIKM '20)*, Mathieu d'Aquin, Stefan Dietze, Claudia Hauff, Edward Curry, and Philippe Cudré-Mauroux (Eds.). Association for Computing Machinery, New York, NY, USA, 2217–2220. <https://doi.org/10.1145/3340531.3412149>

[39] Larissa Capobianco Shimomura, Nikolay Yakovets, and George Fletcher. 2024. Reasoning on property graphs with graph generating dependencies. *Information Sciences* 672 (2024), 120675. <https://doi.org/10.1016/J.INS.2024.120675>

[40] Shaoxu Song, Boge Liu, Hong Cheng, Jeffrey Xu Yu, and Lei Chen. 2017. Graph Repairing under Neighborhood Constraints. *The VLDB Journal* 26, 5 (May 2017), 611–635. <https://doi.org/10.1007/S00778-017-0466-5>

[41] Christopher Spinrath, Angela Bonifati, and Rachid Echahed. 2026. *Repairing Property Graphs under PG-Constraints [Artifacts]*. Zenodo. <https://doi.org/10.5281/zenodo.18301604>

[42] Sławek Staworko, Jan Chomicki, and Jerzy Marcinkowski. 2012. Prioritized Repairing and Consistent Query Answering in Relational Databases. *Annals of Mathematics and Artificial Intelligence* 64, 2–3 (March 2012), 209–246. <https://doi.org/10.1007/s10472-012-9288-8>

[43] Jef Wijsen. 2005. Database repairing using updates. *ACM Transactions on Database Systems* 30, 3 (Sept. 2005), 722–768. <https://doi.org/10.1145/1093382.1093385>

[44] Mingyu Xiao, Sen Huang, and Xiaoyu Chen. 2024. Maximum Weighted Independent Set: Effective Reductions and Fast Algorithms on Sparse Graphs. *Algorithmica* 86, 5 (May 2024), 1293–1334. <https://doi.org/10.1007/s00453-023-01197-x>

[45] Fabian Yamaguchi, Nico Golde, Daniel Arp, and Konrad Rieck. 2014. Modeling and Discovering Vulnerabilities with Code Property Graphs. In *2014 IEEE Symposium on Security and Privacy* (2014-05). IEEE, San Jose, CA, 590–604. <https://doi.org/10.1109/SP.2014.44>

APPENDIX

This appendix consists of three sections. In Appendix appendix:rgpc we provide additional material on RGPC patterns and constraints: We compare RGPC patterns with CRPQs and full GPC in more detail than in Section 6, provide more details on how RGPC constraints can be written as PG-Constraints, provide the formal semantics of predicates, and present a possible extension with reverse traversals of edges. Appendix appendix:repairing provides more details about RGPC automata, the missing proofs for Section 4, as well as an alternative version of the ILP algorithm. Finally, in Appendix C, the interested reader can find additional experimental results together with the raw measurements for all experiments and trade-off percentages.

A RGPC AND RGPC CONSTRAINTS

In Appendices A.1 and A.4 we compare RGPC with CRPQs and full GPC, respectively. And in Appendix A.2 we provide a formal definition for predicates in RGPC constraints. In Appendix A.3 we explain how RGPC can be extended with reverse traversals.

A.1 Relationship to CRPQs

For establishing theoretical foundations, it can be helpful to understand RGPC patterns as extensions of (full) *conjunctive regular path queries* (CRPQ) [see e.g. 6]. A full CRPQ consists of a set of triples (x, r, y) where x and y are node variables, and r is a regular expression over edge labels. A match μ of a triple (x, r, y) in a (property) graph is a mapping that maps x, y to nodes n, m of the graph for which there is a path between n and m such that the *edge labels* of this path form a word in the language of the regular expression r .

For example, $(x, a(bb)^*, y)$ matches all pairs of nodes v_0, v_n for which there is an odd-length path $v_0e_1v_1 \dots e_nv_n$ such that e_1 is labelled a and e_2, \dots, e_n are labelled b . It can be easily translated into an RGPC path pattern, namely $(x) \xrightarrow{:\text{a}} [\xrightarrow{:\text{b}}, \xrightarrow{:\text{b}}]^*(y)$. Other triples (x, r, y) can be translated similarly; and a CRPQ consisting of multiple triples can thus be translated into an RGPC graph pattern. We note that the resulting RGPC patterns *do not* contain any node labels, since the regular expressions r can only refer to edge labels. Furthermore, in an edge pattern $\xrightarrow{:\varphi}$, the label expression φ is always a single label (and does not contain any conjunction, disjunction or negation). Node variables only occur at the beginning and at the end of a path pattern.

A.2 Formal Semantics of Predicates

As stated in Section 3, the semantics of predicates that can occur in the filter and condition of an RGPC constraint is as usual, with the addition that all properties occurring in a predicate must be present. For the sake of completeness, we provide a formal definition below. Recall that \oplus ranges over elements from $\{=, \neq, \leq, \geq\}$. A match μ for an RGPC pattern q in a property graph $G = (N, E, \rho, \lambda, \pi)$ satisfies a predicate ℓ if

- ℓ is of the form $x_i = y_j$ and $\mu(x_i) = \mu(y_j)$;
- ℓ is of the form $x_i \neq y_j$ and $\mu(x_i) \neq \mu(y_j)$;
- ℓ is of the form $x_i \cdot \text{propA} \oplus y_j \cdot \text{propB}$, $\pi(\mu(x_i), \text{propA})$ and $\pi(\mu(y_j), \text{propB})$ are both defined, and

$$\pi(\mu(x_i), \text{propA}) \oplus \pi(\mu(y_j), \text{propB})$$

holds;

- ℓ is of the form $x_i \cdot \text{propA} \oplus c$, $\pi(\mu(x_i), \text{propA})$ is defined, and

$$\pi(\mu(x_i), \text{propA}) \oplus c$$

holds.

A.3 Adding Reverse Traversals

RGPC patterns (and our repair pipeline) can be extended by reverse traversals, i.e. the ability to traverse edges in reverse direction. For this purpose, the definition of paths has to be extended as well, to allow for edges in reverse directions.

Definition A.1 (Path). Let $G = (N, E, \rho, \lambda, \pi)$ be a property graph. A *path* in G is a non-empty alternating sequence $v_0e_1v_1 \dots e_nv_n$ where $v_0, \dots, v_n \in N$ are nodes and $e_1, \dots, e_n \in E$ are edges such that $\rho(e_i) = (v_{i-1}, v_i)$ or $\rho(e_i) = (v_i, v_{i-1})$ holds for every $i \in \{1, \dots, n\}$.

The definition of RGPC can now be augmented with *reverse edge patterns* $\xleftarrow{:\varphi}$. Unlike (forward) edge patterns $\xrightarrow{:\varphi}$, reverse edge patterns require an edge to be traversed in reverse direction in a path to be matched. For example, $\xleftarrow{:\text{a}} \cup \xleftarrow{:\text{c}} \xleftarrow{:\text{c}}$ states that there is an edge labelled a in reverse direction, or a path of length two on which both edges are labelled c .

A.4 RGPC vs. Full GPC

In Section 3 we defined RGPC patterns as a subset of GPC patterns. GPC as defined in the literature [26] has several more features. Notably, it also supports edge variables, and variables to occur below union and repetition operators. This effectively yields two more types of variables, namely optional and group variables, and the semantics become more involved – in the literature a type system is used to determine whether a pattern is valid and define the semantics [26, Section 4]. This is not required for our fragment. Another feature are conditions to match property values. Since property values are covered by the other components of our constraints, namely P and C , we do not require this feature. GPC also allows for traversing edges in the reverse direction or undirected edges. Lastly, path patterns are equipped with restrictors like, for instance, “simple” and “shortest”, which restrict matches to simple paths (no repeated nodes) and shortest paths. The purpose of restrictors is to ensure that there are (only) finitely many matches. This is important if patterns are used to define queries, but constraints do not have a return value. We note that restrictors have also been studied for CRPQs [24].

Lastly, we allow one to specify label constraints using propositional formulas φ . This is not supported by the original definition [26]. Although conjunction and disjunction of labels can be expressed using concatenation and union, expressing the absence of labels (using negation) is, strictly speaking, not possible in the original definition of GPC.

A.5 RGPC Constraints vs. PG-Constraints

As discussed in the introduction, RGPC constraints form a subset of PG-Constraints, which were proposed as an extension of concrete graph query languages, in particular GQL, with constraints [3, 4].

In Section 3, we briefly discussed that the constraint from Example 3.2 is equivalent to the PG-Constraint shown in Figure 1, which uses the **MANDATORY** keyword. Here we provide some more details.

In general, a *PG-Constraint* stipulating mandatory elements is written as

FOR \bar{x} $p(\bar{x})$ **MANDATORY** \bar{y} $q(\bar{x}, \bar{y})$.

Here $p(\bar{x})$ and $q(\bar{x}, \bar{y})$ are queries called the *scope* and *descriptor query*, respectively. They refer to variables $\bar{x} = (x_1, \dots, x_n)$ and $\bar{y} = (y_1, \dots, y_m)$, that are assigned to nodes, paths, or properties.

Example A.2. The PG-Constraint shown in Figure 1, which corresponds to the RGPC constraint from Example 3.2, uses GQL-like scope and descriptor queries. The **MATCH** clause and the first **FILTER** clause form the scope query with free variables x and y . The **MATCH** clause is essentially an ASCII art translation of the RGPC graph pattern in Example 3.2. The first **FILTER** clause asserts that the project has started by comparing the start (date) with the current time.

The **MANDATORY** clause then states that, for every possible match of the **MATCH**-clause’s pattern, it is “mandatory” that the nodes assigned to x and y both have an `access_level` property (more precisely, the records of both nodes are defined for the key `access_level`).

Finally, it is also “mandatory” that the descriptor query, which consists of the second **FILTER**-clause in this example, is satisfied.

The translation in Example A.2 can be generalized to arbitrary constraints $q; F \Rightarrow C$: Every RGPC pattern q can be expressed in GQL [26] and C and F can be written as **FILTER** clauses.

B ADDITIONAL MATERIAL FOR SECTION 4

In Appendix B.1 we provide the formal definition and construction of our automata model for RGPC patterns informally explained in Appendix 4.3. Proofs for Section 4.1 are presented in Appendix section: error-repairing-proofs. In Appendix B.3 we briefly discuss an alternative (which performs worse) to the integer linear programs presented in Section 4.2.

B.1 Automata for RGPC Patterns

Step 2 of our repair pipeline relies on an automata construction, which we detail in the following. We translate RGPC path patterns \mathcal{P} *without node variables* into automata \mathcal{A} which accept precisely those words which are traces of paths matched by \mathcal{P} . For comprehensibility and readability, we assume in the following that \mathcal{P} does not contain any reverse traversals as introduced in Appendix A.3, i.e. (sub-)patterns of the form $\leftarrow \psi$. We will address reverse traversals towards the end of this section.

We start by defining our automata model, which follows the definition of classical symbolic automata, except that there are two sets Q_N and Q_E of states. A state from Q_N indicates that the next transitions reads labels of a node, and a state from Q_E that the next transition reads labels of an edge. We write $\mathcal{B}(S)$ for the set of propositional formulas over a set S of propositions.

Definition B.1 (RGPC Automaton). A (finite) RGPC automaton $\mathcal{A} = (Q_N, Q_E, \mathbf{L}, q_0, \Delta, F)$ consists of

- two finite, disjoint sets Q_N, Q_E of states,
- a finite set \mathbf{L} of labels,
- an *initial state* $q_0 \in Q_N$,

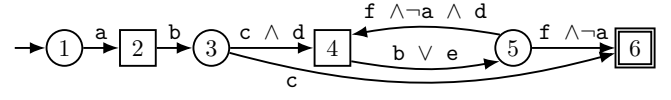


Figure 12: Automaton for the RGPC pattern from Example B.2.

- a finite transition relation

$$\Delta \subseteq (Q_N \times \mathcal{B}(\mathbf{L}) \times Q_E) \cup (Q_E \times \mathcal{B}(\mathbf{L}) \times Q_N),$$

and

- a set $F \subseteq Q_E$ of accepting states.

An RGPC automaton reads words over the alphabet $\Gamma = 2^{\mathbf{L}}$. A *run* of \mathcal{A} on a sequence of label sets $L_1 \dots L_n \in \Gamma^*$ is a sequence $q_0 q_1 \dots q_n$ of states starting with the initial state q_0 such that, for each $i \in \{1, \dots, n\}$, there is a formula φ_i such that $(q_{i-1}, \varphi_i, q_i) \in \Delta$, and $L_i \models \varphi_i$. Here $L_i \models \varphi_i$ holds, if the formula φ_i evaluates to true when interpreting all labels in L_i as variables set to true, and all other labels as variables set to false. A run $q_0 q_1 \dots q_n$ is *accepting* if $q_n \in F$. An RGPC automaton *accepts* a sequence of label sets $L_1 \dots L_n$ if there is an accepting run on that sequence, it *accepts a path* $p = v_0 e_1 v_1 \dots e_n v_n$ of a property graph if it accepts the trace $\lambda(p) = \lambda(v_0)\lambda(e_1)\lambda(v_1) \dots \lambda(e_n)\lambda(v_n)$ of p .

An *automaton for an RGPC path pattern* $z = \mathcal{P}$ is an RGPC automaton \mathcal{A} such that, for every property graph G , \mathcal{A} accepts a path p in G if and only if there is a match μ with $\mu(z) = p$, i.e. p is matched by $z = \mathcal{P}$.

Example B.2. Consider the path pattern

$$(:a) \xrightarrow{:\mathbf{b}} (:\mathbf{c})[(:\mathbf{d}) \xrightarrow{:\mathbf{b} \vee \mathbf{e}} (:\mathbf{f} \wedge \neg a)]^*.$$

The automaton for this path pattern is illustrated in Figure 12.

First, note that the transitions are labelled with propositional formula instead of (single) labels of the property graph. For instance, the transition with the formula $\mathbf{f} \wedge \neg a$ actually represents several transitions: namely, one for each set of labels that contains the label \mathbf{f} but not the label a . In general, computing (and writing) them explicitly would result in an exponential blow-up of the automaton.

For instance, the outgoing transition of state 1 originates from the node pattern $(:a)$, and the outgoing transition of state 2 originates from the edge pattern $\xrightarrow{:\mathbf{b}}$.

We are now prepared to translate an RGPC pattern \mathcal{P} into an RGPC automaton \mathcal{A} for \mathcal{P} . For this purpose, we adapt the standard construction for translating regular expressions into automata: Recall that the automaton reads labels from nodes and edges in alternation, and that consecutive node patterns, without edge patterns in between, match the same node (labels). We observe that RGPC path patterns follow an inductive structure: The base cases are node patterns $(:\varphi)$ and edge patterns $\xrightarrow{\psi}$, and composed patterns are built by combining path patterns using the union, repetition, and concatenation operators. We can thus define \mathcal{A} by induction over the structure of an RGPC path pattern \mathcal{P} . During the construction, we maintain the following invariant: \mathcal{A} has exactly one accepting state q_f , and the accepting state q_f is *not* the initial state q_0 . Furthermore, q_0 has only outgoing transitions and q_f has only incoming transitions. Lastly, let us emphasize that our definition of symbolic automata does *not* permit ϵ -transitions.

Let \mathbf{L} be the set of labels that occur in the pattern \mathcal{P} . The base cases can be translated as follows.

- $\mathcal{P} = (:\varphi)$. A node pattern asserts the existence of a node whose labels satisfy φ . We thus set

$$\mathcal{A} = (\{q_0\}, \{q_f\}, \mathbf{L}, q_0, \{(q_0, \varphi, q_f)\}, \{q_f\}).$$

- $\mathcal{P} = \dashv\varphi$. Next to asserting the existence of an edge, \mathcal{P} also asserts the existence of two nodes, namely the endpoints of the edge. Therefore, we define

$$\begin{aligned} \mathcal{A} = (\{q_0, q_t\}, \{q_s, q_f\}, \mathbf{S}, q_0, \\ \{(q_0, \top, q_s), (q_s, \varphi, q_t), (q_t, \top, q_f)\}, \{q_f\}). \end{aligned}$$

Here \top denotes the tautology which is satisfied by every label set.

Towards the construction for composed path patterns \mathcal{P} , let $\mathcal{A}^1 = (Q_N^1, Q_E^1, \mathbf{L}, q_0^1, \Delta^1, \{q_f^1\})$ and $\mathcal{A}^2 = (Q_N^2, Q_E^2, \mathbf{L}, q_0^2, \Delta^2, \{q_f^2\})$ be the automata constructed for RGPC path patterns \mathcal{P}_1 and \mathcal{P}_2 , respectively. Without loss of generality, we assume that the state sets $Q_N^1, Q_E^1, Q_N^2, Q_E^2$ are pairwise disjoint. We construct an automaton $\mathcal{A} = (Q_N, Q_E, \mathbf{L}, q_0, \Delta, \{q_f\})$ for \mathcal{P} composed of \mathcal{P}_1 and \mathcal{P}_2 .

- $\mathcal{P} = \mathcal{P}_1 \mathcal{P}_2$. Recall that the last node matched by \mathcal{P}_1 corresponds to the first node matched by \mathcal{P}_2 , following the definition of a concatenation of two paths. Therefore, we “merge” the incoming transitions of q_f^1 with the outgoing transitions of q_0^2 .

$$Q_N = Q_N^1 \cup Q_N^2, \quad Q_E = Q_E^1 \cup Q_E^2, \quad q_0 = q_0^1, \quad q_f = q_f^2,$$

$$\Delta = \Delta^1 \cup \Delta^2 \cup \{(q^1, \varphi \wedge \psi, q^2) \mid (q^1, \varphi, q_f^1) \in \Delta^1, (q_0^2, \psi, q^2) \in \Delta^2\}$$

- $\mathcal{P} = \mathcal{P}_1 \cup \mathcal{P}_2$. Since initial states have only outgoing and accepting states only incoming transitions, these transitions can simple be copied for a fresh initial state q_0 and a fresh accepting state q_f .

$$Q_N = Q_N^1 \cup Q_N^2 \cup \{q_0\}$$

$$Q_E = Q_E^1 \cup Q_E^2 \cup \{q_f\},$$

$$\Delta = \Delta^1 \cup \Delta^2 \cup \{(q_0, \varphi, q) \mid (q_0^1, \varphi, q) \in \Delta^1 \text{ or } (q_0^2, \varphi, q) \in \Delta^2\}$$

$$\cup \{(q, \varphi, q_f) \mid (q, \varphi, q_f^1) \in \Delta^1 \text{ or } (q, \varphi, q_f^2) \in \Delta^2\}$$

$$\cup \{(q_0, \varphi, q_f) \mid (q_0^1, \varphi, q_f^1) \in \Delta^1 \text{ or } (q_0^2, \varphi, q_f^2) \in \Delta^2\}$$

- $\mathcal{P} = \mathcal{P}_1^*$. The state sets are $Q_N = Q_N^1 \cup \{q_0\}$ and $Q_E = Q_E^1 \cup \{q_f\}$ where q_0 and q_f are the fresh initial and accepting states, respectively. The transition relation is $\Delta = \Delta^1 \cup \Delta_\varepsilon \cup \Delta_{\geq 1} \cup \Delta_\ell$ where Δ_ε , $\Delta_{\geq 1}$, and Δ_ℓ are defined as follows. The case of \mathcal{P} matching an empty path, i.e. the case of zero repetitions, is covered by Δ_ε . Recall that paths of length zero consists of one node (with an arbitrary label). Thus, we set $\Delta_\varepsilon = \{(q_0, \top, q_f)\}$.

For the other cases the transitions of q_0^1 and q_f^1 are copied to q_0 and q_f .

$$\begin{aligned} \Delta_{\geq 1} = \{(q_0, \varphi, q^1) \mid (q_0^1, \varphi, q^1) \in \Delta^1\} \\ \cup \{(q^1, \varphi, q_f) \mid (q^1, \varphi, q_f^1) \in \Delta^1\} \end{aligned}$$

Finally, we allow the automaton to “loop”. Similar to our construction for the concatenation, transitions have to be merged.

$$\Delta_\ell = \{(q_s^1, \varphi \wedge \psi, q_t^1) \mid (q_s^1, \varphi, q_f^1) \in \Delta^1, (q_0^1, \psi, q_t^1) \in \Delta^1\}$$

Adding Reverse Traversals. For handling reverse traversals, i.e. patterns of the form $\dashv\varphi$, we will understand the direction of an edge as an additional label. More precisely, we consider two special labels fw and bw for forward and reverse traversals, respectively, which do not occur in the pattern \mathcal{P} (or the underlying property graph). For a pattern $\dashv\varphi$, we then construct the transition $(q_s, \text{fw} \wedge \varphi, q_t)$ instead of (q_s, φ, q_t) . The automaton for a pattern $\dashv\psi$ can then be constructed analogously, yielding in the transition $(q_s, \text{bw} \wedge \varphi, q_t)$. Observe that label expressions of transitions for edge patterns are never combined in the overall construction (only label expressions for node labels are). Consequently, all outgoing transitions of states in Q_E , i.e. states that indicate that the next transitions reads labels of an edge, have either label expressions of the form $\text{fw} \wedge \varphi$ or of the form $\text{bw} \wedge \varphi$, where φ and ψ contain neither fw nor bw. Outgoing transitions of states in Q_N do not contain the special labels fw and bw at all, since they read only node labels.

For adapting the semantics, we define the *extended trace* of a path $P = v_0 e_1 v_1 \dots e_n v_n$ as

$$\lambda^*(P) = \lambda(v_0) \lambda^*(v_0, e_1, v_1) \lambda(v_1) \dots \lambda^*(v_{n-1}, e_n, v_n) \lambda(v_n),$$

where $\lambda(v_i)$ is, as before, the set of labels of node v_i , and

$$\lambda^*(v_{i-1}, e_i, v_i) = \begin{cases} \lambda(e_i) \cup \{\text{fw}\}, & \text{if } \rho(e_i) = (v_{i-1}, v_i), \\ \lambda(e_i) \cup \{\text{bw}\}, & \text{if } \rho(e_i) = (v_i, v_{i-1}) \end{cases}$$

extends the set $\lambda(e_i)$ of labels of an edge e_i by either fw or bw, depending on whether e_i is traversed in a forward or reverse fashion in the path P .

An RGPC automaton (with reverse traversals) then accepts a path $P = v_0 e_1 v_1 \dots e_n v_n$ if it accepts the extended trace $\lambda^*(P)$ of that path.

B.2 Error Repairing

This section is dedicated to the proofs of Propositions 4.7 and 4.8.

PROOF OF PROPOSITION 4.7. Let Σ be a set of RGPC constraints, G be a property graph, and V be a minimum weight vertex cover of the (topological) conflict hypergraph of G w.r.t. Σ . Furthermore, let G' be the subgraph of G obtained by removing all nodes and edges in V , as well as all edges incident to the nodes in V . We prove that G' is a repair by showing that conditions a) and b) from Definition 4.3 hold by contradiction.

For the sake of contradiction assume that Condition a) does not hold, that is G' violates a constraint $q; F \Rightarrow C$ from Σ . Then there is a match μ of q in G' . Let O_μ be the topological error induced by μ . Since all nodes and edges of G' also appear in G' with the same labels and properties – G' is a topological subgraph – O_μ is also a topological error of G . But then it is also a hyperedge of the conflict hypergraph of G , and since all its elements are still present in G' , its intersection with V is empty. This is a contradiction to V being a vertex cover. We conclude that Condition a) holds.

For proving that Condition b) holds, we assume, again for the sake of contradiction, that there is a subgraph G'' of G such that G'

is a proper subgraph of G'' and G'' satisfies all constraints from Σ . Then there is a node or edge o in G'' that is not present in G' . We make a case distinction.

In case $o \in V$, consider all topological errors O_1, \dots, O_m of G containing object o . Since G'' satisfies all constraints, there are objects $o_1 \in O_1, \dots, o_m \in O_m$, which are distinct from o , and not present in G'' . But since G' is a subgraph of G'' , the objects o_1, \dots, o_m are also not present in G' . Furthermore, we can assume that every o_j is in V : If not, then o_j is an edge which was removed because one of its endpoints, say a node n , was removed. But then O_j also contains n , since errors originate from paths. Moreover, n cannot be o because the weight of n is higher than the sum of the weights of its incident edges, and hence higher than the sum of weights of all o_j not in V . Consequently, n being in V but some edges o_j not being in V would contradict V having minimum weight. Therefore, we can indeed assume that o_j is n , and hence in V . In addition, since all o_j are in V , we can conclude that $V \setminus \{o\}$ is a vertex cover. And since it has a lesser weight than V this contradicts the fact that V is a minimal vertex cover.

It remains to consider the case $o \notin V$. Then o is an edge that was removed because one of its endpoints n was removed due to being in V . Since G'' contains o , it also has to contain its endpoint n . Therefore, applying the first case for $n \in V$ yields a contradiction.

Overall, we can conclude that Condition b) holds. \square

PROOF OF PROPOSITION 4.8. We proceed similarly as in the proof of Proposition 4.7. Let Σ be a set of RGPC constraints, G be a property graph, and V_g be a minimum vertex cover of the (topological) conflict hypergraph of G w.r.t. Σ , computed by the greedy algorithm. Furthermore, let G' be the subgraph of G obtained by removing all nodes and edges from V_g , as well as all edges incident to nodes in V_g . We prove that G' is a repair by showing that conditions a) and b) from Definition 4.3 hold. The proof of Condition a) being satisfied is exactly the same as in the proof for Proposition 4.7, since it only relies on V_g being a vertex cover.

To prove that Condition b) holds, we assume, for the sake of contradiction, that there is a subgraph G'' of G such that G' is a proper subgraph of G'' and G'' satisfies all constraints from Σ . Then there is a node or edge o in G'' that is not present in G' .

In case $o \in V_g$, consider all topological errors O_1, \dots, O_m of G with $V_g \cap O_i = \{o\}$. Note that there is at least one such O_i , because otherwise o would have been removed from V_g in the second phase of the greedy algorithm. Furthermore, for at least one of these errors O_j we have that o is the object with the least weight among all objects in O_j . If this would not be the case, the greedy algorithm would have picked elements $o_1 \in O_1, \dots, o_m \in O_m$ with a smaller weight than o in the first phase and consequently removed o from V_g in the second phase prior to removing o_1, \dots, o_m , since o has a greater weight. We fix one of these errors O_j for which o has minimal weight among the objects in O_j . Since $V_g \cap O_j = \{o\}$, all objects $O_j \setminus \{o\}$ are in G' , and hence also in G'' since G' is a subgraph of G'' . Note that this is particularly true if o is a node: Since o has minimal weight, O_j cannot contain an edge in that case. But since G'' also contains o , it contains all objects of O_j . This is a contradiction because O_j originates from a match μ of the pattern q of a constraint $q; F \Rightarrow C$ in Σ that passes F but does not satisfy C . Thus, G'' violates the constraint.

It remains to consider the case $o \notin V_g$. Then o is an edge that was removed because one of its endpoints n was removed due to being in V_g . Since G'' contains o , it also has to contain its endpoint n . Therefore, applying the first case for $n \in V_g$ yields a contradiction.

Overall, we can conclude that Condition b) holds. \square

B.3 ILPs with Explicit Dependencies

In this section, we discuss an alternative to the ILPs presented in Section 4.1, and why we did *not* choose it. Thanks to the use of weights in the ILPs presented in Section 4.1, it is ensured that nodes are only deleted if necessary, and deleting (a subset of its) incident edges takes precedence. One potential issue with this approach is, however, that the weights are *static* (i.e. hardcoded in the ILP): For example, consider a constraint that forbids the presence of two different nodes with the same value for the name property. Suppose there are two nodes n_1, n_2 with two and five incident edges, respectively, violating this constraint. Since n_1 has weight 3 and n_2 weight 6, an ILP solver will always mark n_1 for deletion. This is, in particular, true even if, due to another constraint, the ILP also marked all incident edges of n_2 for deletion (and no incident edge of n_1). But in this case, the “effective weight” of n_2 is only 1, and thus n_2 should be marked for deletion instead of n_1 . This can be addressed by constructing and solving an alternative ILP, in which dependencies are encoded explicitly. That is, if n_1 has the two incident edges e_1 and e_2 in the property graph, then we add the constraint $2x_{n_1} \leq x_{e_1} + x_{e_2}$ to the ILP. Thanks to this constraint, the variables for x_{e_1} and x_{e_2} for the edges have to be assigned value 1 in a solution whenever the variable x_{n_1} for n_1 is assigned value 1 (recall that value 1 means that the object is deleted). Weights are then no longer necessary and the ILP takes the following form, where E_n is the set of incident edges of a node $n \in N$ of the property graph.⁹

$$\begin{aligned} \text{minimize} \quad & \sum_{v \in \mathcal{W}} x_v \\ \text{subject to} \quad & \sum_{v \in O} x_v \geq 1 \quad \text{for all } O \in \mathcal{E} \\ & |E_n| \cdot x_n \leq \sum_{e \in E_n} x_e \quad \text{for all } n \in N \cap \mathcal{W} \\ & 0 \leq x_v \leq 1 \quad \text{for all } v \in \mathcal{W} \end{aligned}$$

This variant trades a larger ILP for a *potentially* better repair. However, in our experiments, it took significantly longer to solve the ILP with explicit dependencies in all cases, while the repairs obtained were the same as for the ILP with weights.

C ADDITIONAL MATERIAL FOR EXPERIMENTS

In Appendix C.1 we present plots for combinations of optional steps/datasets/constraints not shown in Section 5. Appendix C.2 contains the raw numbers used for the plots, as well as the runtime increase and deletion reduction percentages, in particular those reported in the paper.

⁹Strictly speaking, the elements of each E_n with $n \in \mathcal{W}$ have to be added to the set \mathcal{W} of vertices of the conflict hypergraph.

C.1 Additional Experimental Results

We provide additional plots akin to those in Section 5, for the remaining combinations of optional steps/datasets/constraints.

Scaling. In Section 5.1 we provide plots for showcasing how the base pipeline scales on the ICIJ and LDBC graphs with 1-way constraints. Figure 13 shows similar plots for the legislative and Coreutils datasets. As observed in the paper for the ICIJ and LDBC datasets, the number of deletions is comparatively small, and the pipeline scales well.

We also performed scaling experiments for 1-way constraints with Step 2 enabled. Figures 17 and 18 show the runtime and number of label deletions, if Step 2 is enabled. They assert that, as for the base pipeline, our pipeline performs well when the number of required deletions is small if Step 2 is enabled, although the runtime is consistently higher than for the base pipeline, confirming our observations in Section 5.3.

Approximate Repairs. In Section 5.1 we investigated the approximate repairs yielded by the selection phase of the naive and LP-guided greedy algorithms. For the ICIJ graph we discussed that the selection phase of the naive greedy performs generally better than the one for the LP-guided greedy algorithm, but overall the naive greedy algorithm performs worse, since it has to trim more objects in the trimming phase. The same applies to the other datasets as shown in Figures 15 and 16, and in comparison with Figures 6a, 6b, 6c, and 6d, which show total runtime, and Figures 7a, 7b, 7c, and 7d, which show the edge deletions, in the paper for the full algorithms computing repairs. As for the ICIJ dataset in the paper, we can also observe that the LP-guided greedy algorithms often achieves optimal quality (and thus actually computes a repair), while the naive greedy does not. However, when the naive greedy comes close to an optimal solution in the selection phase, it can outperform the LP-guided greedy when computing a repair (and not only an approximation).

Minimizing Deletions of Important Objects. In Section 5.2 we assessed the robustness of our pipeline with respect to custom weights. More precisely, we used the PageRank scores for nodes and edges as custom weights for repairing the ICIJ graph, and discussed that the weight loss of a repair can be reduced by 24% when using custom weights. This indicates that more important edges, i.e. edges with a high PageRank score, are preserved. Table 3 shows the total weights, weight losses, and loss reductions for all sets of constraints. The loss reduction is computed as

$$100 \cdot \left(1 - \frac{w_{\text{orig}} - w_{\text{cw-repair}}}{w_{\text{orig}} - w_{\text{repair}}} \right)$$

where w_{orig} is the total weight of the input graph, $w_{\text{cw-repair}}$ is the total weight of a repair when custom weights are provided, and w_{repair} is the total weight of a repair when no custom weights are provided. For 2-rep constraints the loss reduction is even 46%, albeit the weight loss is lower for repairs without custom weights than for the case of 1-way constraints discussed in the paper.

Table 3 also shows the experimental results for the Coreutils graph, and Figures 14a and 14b show the runtime and edge deletions for the Coreutils graph when PageRank scores are provided as

custom weights. Compared with Figures 6b and 7b in the paper they confirm our findings for the ICIJ graph.

We used the Graph Data Science Library of Neo4j to compute the PageRank scores. Since PageRank scores are, as usual, computed for nodes, we computed the PageRank scores for edges using line graphs, in which the role of nodes and edges is, intuitively, swapped: The *line graph* $G_L = (V_L, E_L)$ of a graph $G = (V, E)$ is the graph with $V_L = E$, and a pair $(e_1, e_2) \in V_L \times V_L$ is in E_L if and only if there are $v_0, v_1, v_2 \in V$ such that $v_0 e_1 v_1 e_2 v_2$ is a path in G . For the legislative and LDBC graph computing the line graph for computing edge weights was not possible with our hardware using Neo4j.

Step 2/Label Deletions. Figure 19 shows the runtimes and number of edge deletions of our repair pipeline with Step 2 enabled for the Coreutils and LDBC datasets and the sets of constraints outlined in Table 1. Compared to the corresponding plots for the base pipeline in Section 5.4, they provide the same insight as the analogous plots for the legislative and ICIJ graphs discussed in Section 5.3: With Step 2 enabled the repair pipeline yields higher-quality repairs (measured in the number of deletions), at the expense of a higher runtime.

Step 3/Neighbourhood Errors. Figures 20, 21, 21, and 23 show the plots for the neighbourhood error repairs (Step 3), except for the combination of ICIJ graph and the LP-guided greedy algorithm, for which they are shown in Section 5.3. They are supporting our insights discussed in Section 5.3: If k is chosen well, a runtime improvement can be achieved in almost all cases, while retaining a high quality. For 2-rep constraints (which are only available for the ICIJ and LDBC graphs), $k = 4$ yields a quality close (or identical) to the base pipeline, while for the other constraints $k = 2$ already suffices. This effect can be explained by the shape of our constraints: The minimal length of a path within a match of the 2-rep constraints is 9, while it is at most 6 for the other constraints. For matches where all paths are of length at most 6 the complete match is within the 4-neighbourhood, and the 2-neighbourhood covers most of it. Furthermore, since our constraints exhibit repetitions, it is likely that larger errors are resolved by repairing smaller ones, in particular those containing paths of length at most 6. For 2-rep constraints, the 4-neighbourhood covers matches with minimal-length paths almost completely but the 2-neighbourhood does not, explaining why for $k = 4$ the result is very close to the base case, and worse for $k = 2$ in this case. This suggests that a good choice for k is $k = \frac{\ell_{\min}}{2}$ where ℓ_{\min} is the minimal length of a path matched by a path pattern of the constraint.

Another noteworthy observation is that the naive greedy algorithm can yield a better quality with Step 3 enabled than without. For example, this happens for 1-way constraints and $k = 4$ for the legislative graph (Figure 20d vs. Figure 7a in the paper). The underlying reason is that the naive greedy selects *any* object from an error for removal: Truncating an error can thus change which object is selected and can lead to a higher-quality repair (but also to lower-quality repairs in others). For the LP-guided greedy and ILP strategies we cannot observe this effect, since these strategies can better avoid bad selections thank to the (I)LP solutions.

Finally, Figure 24 shows the results when running the pipeline with random samples of $2k$ edges from each topological error, except

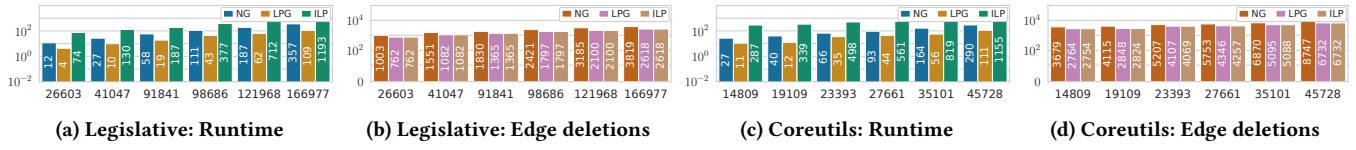


Figure 13: Runtime and number of edge deletions for LDBC and the Coreutils graph for subsets of 1-way constraints

Table 3: Total edge weight for repairs proposed by the LP-guided greedy algorithm when the pipeline does or does not use the custom weights. Here the weight of an edge is its PageRank in the line graph. For readability all weights are rounded.

Dataset	Shape	Original Weight	Repair w/o custom weights		Repair with custom weights		
			Repair Weight	Weight Loss	Repair Weight	Weight Loss	Loss Reduction
ICIJ	1-way	579593.37	579060.61	0.0919%	579188.60	0.0698%	24%
	2-way		579233.32	0.0621%	579261.99	0.0572%	7%
	2-rep		579548.82	0.0077%	579569.60	0.0041%	46%
	loop		579143.61	0.0776%	579219.41	0.0645%	16%
	3-split		579590.94	0.0004%	579590.94	0.0004%	0%
Coreutils	1-way	112369.10	110873.74	1.3308%	110920.13	1.2895%	3%
	2-way		112203.69	0.1472%	112225.11	0.1281%	13%



Figure 14: Runtimes (in seconds) and deletions for the Coreutils graph when using PageRank scores as custom weights

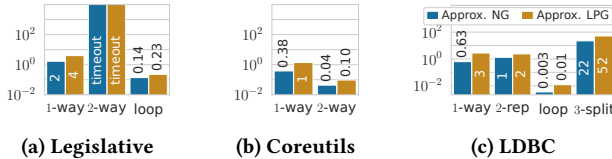


Figure 15: Runtimes in seconds of the selection phase of the naive greedy (NG) and LP-guided greedy (LPG)

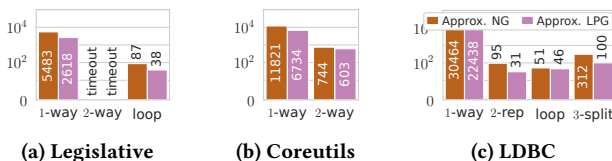


Figure 16: Number of edge deletions of the selection phase of the naive greedy (NG) and LP-guided greedy (LPG)

for the ICIJ graph, for which they are shown in Section 5.3 in the paper. They confirm our observation discussed in the paper for the ICIJ graph: taking random samples can result in significantly more deletions. We conclude that picking neighbourhoods around path endpoints is a more appropriate strategy.

C.2 Raw Measurements and Trade-Off Percentages

Table 4 shows the runtimes recorded for the datasets and sets of constraints listed in Table 1 for the base pipeline and with Step 2 (label deletions) enabled in the fourth and sixth column, respectively. All numbers are averages of four runs. Column 5 contains the runtime reduction, in percentage, achieved for the base pipeline by the naive greedy and the LP-guided greedy algorithms relative to the ILP algorithm. To be precise, the runtime reduction is

$$100 \cdot \frac{r_{\text{ilp}} - r_g}{r_{\text{ilp}}},$$

where r_{ilp} is the runtime of the ILP algorithm, and r_g is the runtime of the naive or LP-guided greedy algorithm. For instance, the first three rows state that, for 1-way constraints on the Coreutils graph, the runtime of the naive greedy algorithm is 74.86% less than the reference value 1154.86s for the ILP algorithm, and the LP-guided greedy algorithm even achieves a runtime reduction of 90.13%.

Similarly, the last column shows the runtime *increase*

$$100 \cdot \frac{r_{\text{label}}}{r_{\text{base}}},$$

when enabling Step 2. Here r_{base} is the runtime of the naive greedy, LP-guided greedy, or ILP algorithm for the base pipeline, and r_{label} the runtime with Step 2 enabled. For example, the first row states that the naive greedy algorithm takes 290.32s for the base pipeline, and with Step 2 enabled, it takes 320.46s, which is 110.38% of the reference value 290.32s. Extrema, and in particular numbers reported in the main paper, are printed in bold face in a (blue) frame. Tables 10 and 11 show the corresponding numbers for the scaling plots, and Table 15 for the selection phase of the greedy algorithms to compute approximate repairs, as discussed in Section 5.1 and Appendix C.1. For the experiments with custom weights in Section 5.2 and Appendix C.1, they are shown in Table 14.

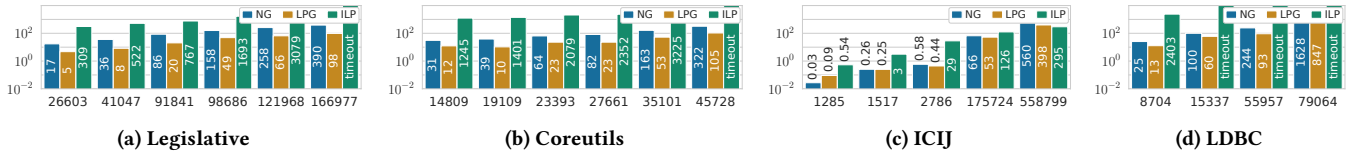


Figure 17: Runtimes of the repair pipeline with Step 2 (label deletions) enabled for subsets of 1-way constraints

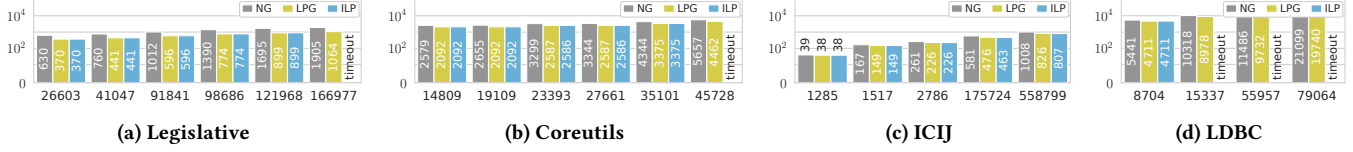


Figure 18: Label deletions proposed by the repair pipeline with Step 2 (label deletions) enabled for subsets of 1-way constraints

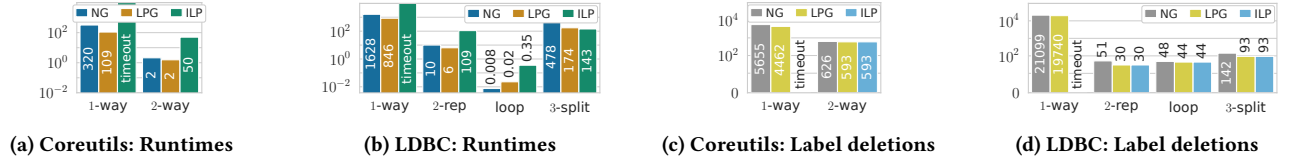


Figure 19: Runtime with Step 2 enabled and number of label deletions for the Coreutils graph and LDBC

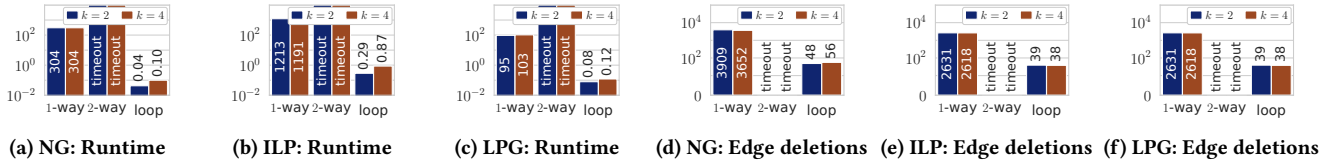


Figure 20: Runtime (in seconds) and edge deletions for neighbourhood errors for the legislative graph

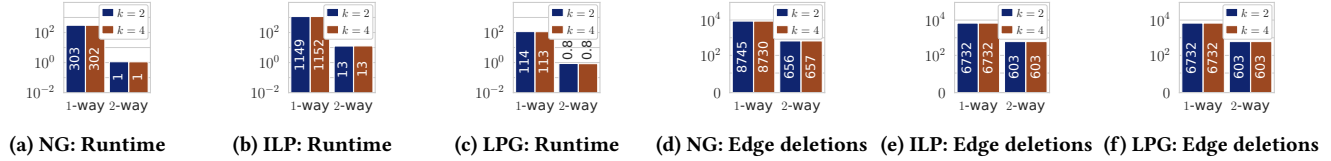


Figure 21: Runtime (in seconds) and edge deletions for neighbourhood errors for the Coreutils graph

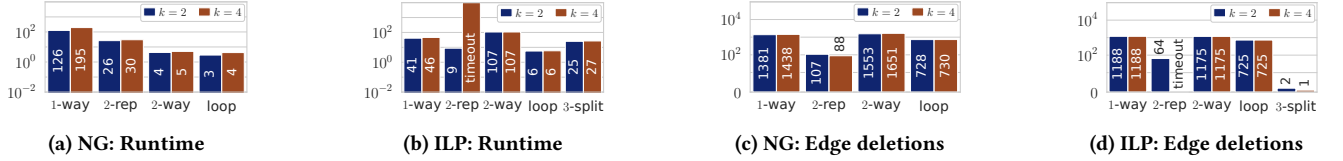


Figure 22: Runtime (in seconds) and edge deletions for neighbourhood errors for the ICIJ graph

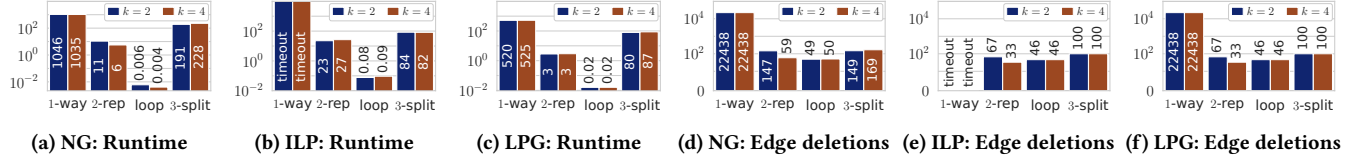


Figure 23: Runtime (in seconds) and edge deletions for neighbourhood errors for the LDBC graph

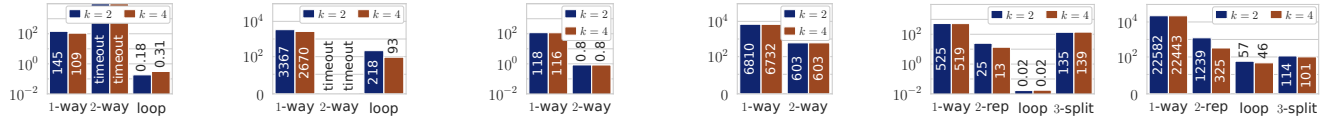


Figure 24: Runtimes (in seconds) and edge deletions for sample errors of the LP-guided greedy algorithm

Table 5 show the recorded numbers of deletions for the base pipeline and with Step 2 enabled. For example, the first three rows of Table 5 show that the naive greedy algorithm yields 8747 edge deletions, and the LP-guided greedy and ILP algorithm both yield 6732 edge deletions for the base pipeline. That is, the LP-guided greedy and ILP strategies yield 23.04% less deletions, which is reported in the fifth column, and hence a higher quality. In general, the reduction in deletions is calculated as

$$100 \cdot \frac{d_{ng} - d_{lp}}{d_{ng}},$$

where d_{ng} is the number of edge deletions yielded by the naive greedy algorithm, and d_{lp} the number of deletions yielded by the LP-guided greedy or ILP strategy. The last column shows the reduction (or quality gain) in the number of deletions with Step 2 enabled, calculated by

$$100 \cdot \frac{d_{base} - d_{label}}{d_{base}},$$

where d_{base} is the number of edge deletions yielded by the base pipeline, and d_{label} is the number of label deletions yielded with Step 2 enabled. For example, the first row states that, with Step 2 enabled, the naive greedy algorithm opts for deleting about 5655 labels (column 6), which is 35.35% less than the reference value of 8747 edge deletions in column 4. As for the runtime table, all

values are averaged over four runs. Since the greedy algorithms can pick a different number of deletions in each run, the average is not necessarily an integer value. Tables 12 and 13 shows the number of deletions for the scaling experiments and Table 16 for the approximate repairs discussed in Section 5.1 and Appendix C.1. For the experiments with custom weights in Section 5.2 and Appendix C.1, they are shown in Table 14.

Table 6 shows the runtimes and runtime reductions over the base pipeline for Step 3 (neighbourhood error repairs); analogously to Table 4 explained above. The runtime reductions are computed with the formula

$$100 \cdot \frac{r_{base} - r_{nbh}}{r_{base}},$$

where r_{nbh} and r_{base} are the runtimes with and without Step 3 enabled, respectively. The runtime (reductions) for the experiments in Section 5.3 with sampled errors are shown in Table 8.

Finally, Table 7 shows the deletions with and without Step 3 enabled. The percentage is computed as

$$100 \cdot \frac{d_{nbh}}{d_{base}},$$

where d_{nbh} and d_{base} are the numbers of deletions with Step 3 enabled and without Step 3, respectively. The numbers of edge deletions for the experiments in Section 5.3 with sampled errors are shown in Table 9.

Table 4: Raw runtimes and runtime comparisons for the datasets and sets of constraints listed in Table 1

Dataset	Shape	#Errors	Algorithm	Base Pipeline		Repair with label deletions (Step 2)	
				Runtime	Runtime Reduction	Runtime	Runtime Increase
Coreutils	1-way	45728	Naive Greedy	290.32	74.86	320.46	110.38
	1-way	45728	LP-Guided Greedy	113.95	90.13	109.13	95.78
	1-way	45728	ILP	1154.86			
	2-way	3707	Naive Greedy	1.11	91.19	2.11	190.02
	2-way	3707	LP-Guided Greedy	0.85	93.24	1.56	182.73
	2-way	3707	ILP	12.59		49.92	396.47
Legislative	1-way	166977	Naive Greedy	356.64	70.10	389.81	109.30
	1-way	166977	LP-Guided Greedy	111.94	90.62	97.90	87.46
	1-way	166977	ILP	1192.84			
	2-way	419439	Naive Greedy				
	2-way	443695	LP-Guided Greedy				
	2-way	419439	ILP				
	loop	3783	Naive Greedy	0.18	86.57	0.22	126.09
	loop	3783	LP-Guided Greedy	0.28	78.61	0.56	200.18
ICIJ	loop	3783	ILP	1.31		4.37	334.05
	1-way	558799	Naive Greedy	324.12	-445.65	559.79	172.71
	1-way	558799	LP-Guided Greedy	183.48	-208.89	393.31	214.36
	1-way	558799	ILP	59.40		294.69	496.11
	2-rep	397108	Naive Greedy	35.68		53.62	150.28
	2-rep	397108	LP-Guided Greedy	45.27			
	2-rep	397108	ILP				
	2-way	7553	Naive Greedy	4.89	95.51	6.52	133.22
	2-way	7553	LP-Guided Greedy	2.34	97.85	3.75	159.83
	2-way	7553	ILP	108.90		429.15	394.07
LDBC	loop	56614	Naive Greedy	6.14	10.13	14.69	239.29
	loop	56614	LP-Guided Greedy	7.51	-9.97	16.04	213.45
	loop	56614	ILP	6.83		23.21	339.75
	3-split	876933	Naive Greedy	3.03	89.02	4.11	135.57
	3-split	876933	LP-Guided Greedy	25.98	5.91	54.69	210.54
	3-split	876933	ILP	27.61		56.13	203.29
	1-way	79064	Naive Greedy	980.82		1627.58	165.94
	1-way	79064	LP-Guided Greedy	527.74		846.50	160.40
	1-way	79064	ILP				
	2-rep	72756	Naive Greedy	3.90	86.29	9.99	256.01
LDBC	2-rep	72756	LP-Guided Greedy	3.36	88.18	6.35	188.79
	2-rep	72756	ILP	28.46		109.26	383.86
	loop	423	Naive Greedy	0.0041	95.97	0.01	182.72
	loop	423	LP-Guided Greedy	0.01	86.28	0.02	162.33
	loop	423	ILP	0.10		0.35	347.20
	3-split	1358499	Naive Greedy	225.46	-165.99	477.74	211.90
	3-split	1358499	LP-Guided Greedy	87.64	-3.40	173.72	198.22
	3-split	1358499	ILP	84.76		143.25	169.00

Table 5: Raw number of deletions and comparisons for the datasets and sets of constraints listed in Table 1

Dataset	Shape	#Errors	Algorithm	Base Pipeline		Repair with label deletions (Step 2)	
				#Edge Deletions	Reduction in Deletions	#Label Deletions	Delete Reduction
Coreutils	1-way	45728	Naive Greedy	8747.00		5655.29	35.35
	1-way	45728	LP-Guided Greedy	6732.00	23.04	4462.00	33.72
	1-way	45728	ILP	6732.00	23.04		
	2-way	3707	Naive Greedy	656.00		626.33	4.52
	2-way	3707	LP-Guided Greedy	603.00	8.08	593.00	1.66
	2-way	3707	ILP	603.00	8.08	593.00	1.66
Legislative	1-way	166977	Naive Greedy	3818.67		1905.33	50.10
	1-way	166977	LP-Guided Greedy	2618.00	31.44	1064.33	59.35
	1-way	166977	ILP	2618.00	31.44		
	2-way	419439	Naive Greedy				
	2-way	443695	LP-Guided Greedy				
	2-way	419439	ILP				
	loop	3783	Naive Greedy	49.67		32.33	34.90
	loop	3783	LP-Guided Greedy	38.00	23.49	20.00	47.37
	loop	3783	ILP	38.00	23.49	20.00	47.37
ICIJ	1-way	558799	Naive Greedy	1411.00		1008.33	28.54
	1-way	558799	LP-Guided Greedy	1188.33	15.78	826.33	30.46
	1-way	558799	ILP	1188.00	15.80	807.00	32.07
	2-rep	397108	Naive Greedy	79.67		57.00	28.45
	2-rep	397108	LP-Guided Greedy	50.67	36.40		
	2-rep	397108	ILP				
	2-way	7553	Naive Greedy	1588.33		1261.00	20.61
	2-way	7553	LP-Guided Greedy	1176.33	25.94	1072.00	8.87
	2-way	7553	ILP	1175.00	26.023	1072.00	8.77
	loop	56614	Naive Greedy	727.33		720.67	0.92
	loop	56614	LP-Guided Greedy	725.00	0.32	715.33	1.33
	loop	56614	ILP	725.00	0.32	715.00	1.38
	3-split	876933	Naive Greedy	2.00		1.00	50.00
	3-split	876933	LP-Guided Greedy	1.00	50.0	1.00	0.00
	3-split	876933	ILP	1.00	50.0	1.00	0.00
LDBC	1-way	79064	Naive Greedy	22438.00		21099.00	5.97
	1-way	79064	LP-Guided Greedy	22438.00		19740.00	12.02
	1-way	79064	ILP				
	2-rep	72756	Naive Greedy	42.33		51.33	-21.26
	2-rep	72756	LP-Guided Greedy	31.00	26.77	30.00	3.23
	2-rep	72756	ILP	31.00	26.77	30.00	3.23
	loop	423	Naive Greedy	48.67		48.00	1.37
	loop	423	LP-Guided Greedy	46.00	5.48	44.00	4.35
	loop	423	ILP	46.00	5.48	44.00	4.35
	3-split	1358499	NG	155.00		142.33	8.17
	3-split	1358499	LPG	100.00	35.48	93.00	7.00
	3-split	1358499	ILP	100.00	35.48	93.00	7.00

Table 6: Raw runtimes and runtime comparisons for Step 3 (neighbourhood errors)

Dataset	Shape	#Errors	Algorithm	Base Pipeline		k = 2		k = 4	
				Runtime	Runtime	Runtime	Runtime Reduction	Runtime	Runtime Reduction
Coreutils	1-way	45728	Naive Greedy	290.32	302.98	-4.36		301.72	-3.93
	1-way	45728	LP-Guided Greedy	113.95	114.42	-0.42		113.00	0.83
	1-way	45728	ILP	1154.86	1148.77	0.53		1152.01	0.25
	2-way	3707	Naive Greedy	1.11	1.13	-1.77		1.12	-0.61
	2-way	3707	LP-Guided Greedy	0.85	0.87	-1.6445		0.84	1.01
	2-way	3707	ILP	12.59	12.54	0.41		12.76	-1.32
Legislative	1-way	166977	Naive Greedy	356.64	304.48	14.63		303.79	14.82
	1-way	166977	LP-Guided Greedy	111.94	95.14	15.00		102.70	8.25
	1-way	166977	ILP	1192.84	1213.44	-1.73		1190.86	0.17
	2-way	443695	Naive Greedy						
	2-way	443695	LP-Guided Greedy						
	2-way	443695	ILP						
	loop	3783	Naive Greedy	0.18	0.04	75.99		0.10	43.61
	loop	3783	LP-Guided Greedy	0.28	0.08	71.90		0.12	57.24
	loop	3783	ILP	1.31	0.29	78.04		0.87	33.86
ICIJ	1-way	558799	Naive Greedy	324.12	126.14	61.08		194.55	39.98
	1-way	558799	LP-Guided Greedy	183.48	68.21	62.83		103.09	43.81
	1-way	558799	ILP	59.40	41.21	30.62		46.21	22.21
	2-rep	397108	Naive Greedy	35.68	26.33	26.20		30.24	15.26
	2-rep	397108	LP-Guided Greedy	45.27	9.19	79.69		44.98	0.63
	2-rep	397108	ILP		8.78				
	2-way	7553	Naive Greedy	4.89	4.33	11.53		5.07	-3.60
	2-way	7553	LP-Guided Greedy	2.34	2.27	3.35		2.47	-5.12
	2-way	7553	ILP	108.90	106.91	1.83		107.20	1.57
	loop	56614	Naive Greedy	6.14	2.90	52.84		4.23	31.08
	loop	56614	LP-Guided Greedy	7.51	3.50	53.42		5.01	33.36
	loop	56614	ILP	6.83	5.66	17.21		5.87	14.03
	3-split	876933	Naive Greedy	3.03	4.46	-47.12		2.01	33.65
	3-split	876933	LP-Guided Greedy	25.98	23.84	8.24		25.79	0.74
	3-split	876933	ILP	27.61	25.35	8.19		26.83	2.84
LDBC	1-way	79064	Naive Greedy	980.82	1045.71	-6.62		1034.62	-5.48
	1-way	79064	LP-Guided Greedy	527.74	519.94	1.48		524.52	0.61
	1-way	79064	ILP						
	2-rep	72756	Naive Greedy	3.90	10.76	-175.78		5.58	-42.98
	2-rep	72756	ILP	28.46	22.60	20.61		26.62	6.47
	loop	423	Naive Greedy	0.0041	0.006	-46.73		0.0041	1.02
	loop	423	LP-Guided Greedy	0.01	0.06	-13.40		0.02	-14.46
	loop	423	ILP	0.10	0.08	24.36		0.09	8.13
	3-split	1358499	Naive Greedy	225.46	191.02	15.2738		227.6318	-0.9631
	3-split	1358499	LP-Guided Greedy	87.64	79.87	8.86		87.07	0.65
	3-split	1358499	ILP	84.76	83.97	0.93		82.45	2.73

Table 7: Raw edge deletions and deletion comparisons for Step 3 (neighbourhood errors)

Dataset	Shape	#Errors	Algorithm	Base Pipeline		k = 2		k = 4	
				Deletions	Deletions	Percentage	Deletions	Deletions	Percentage
Coreutils	1-way	45728	Naive Greedy	8747.00	8744.67	99.97	8730.00	8730.00	99.81
	1-way	45728	LP-Guided Greedy	6732.00	6732.00	100.00	6732.00	6732.00	100.00
	1-way	45728	ILP	6732.00	6732.00	100.00	6732.00	6732.00	100.00
	2-way	3707	Naive Greedy	656.00	656.00	100.00	656.67	656.67	100.10
	2-way	3707	LP-Guided Greedy	603.00	603.00	100.00	603.00	603.00	100.00
	2-way	3707	ILP	603.00	603.00	100.00	603.00	603.00	100.00
Legislative	1-way	166977	Naive Greedy	3818.67	3909.33	102.37	3652.00	3652.00	95.64
	1-way	166977	LP-Guided Greedy	2618.00	2631.00	100.50	2618.00	2618.00	100.00
	1-way	166977	ILP	2618.00	2631.00	100.50	2618.00	2618.00	100.00
	2-way	443695	Naive Greedy						
	2-way	443695	LP-Guided Greedy						
	2-way	443695	ILP						
	loop	3783	Naive Greedy	49.67	48.33	97.32	56.00	56.00	112.75
	loop	3783	LP-Guided Greedy	38.00	39.00	102.63	38.00	38.00	100.00
	loop	3783	ILP	38.00	39.00	102.63	38.00	38.00	100.00
ICIJ	1-way	558799	Naive Greedy	1411.00	1381.33	97.90	1438.33	1438.33	101.94
	1-way	558799	LP-Guided Greedy	1188.33	1188.33	100.00	1188.33	1188.33	100.00
	1-way	558799	ILP	1188.00	1188.00	100.00	1188.00	1188.00	100.00
	2-rep	397108	Naive Greedy	79.67	107.33	134.73	88.33	88.33	110.88
	2-rep	397108	LP-Guided Greedy	50.67	64.00	126.32	56.00	56.00	110.53
	2-rep	397108	ILP		64.00				
	2-way	7553	Naive Greedy	1588.33	1552.67	97.75	1650.67	1650.67	103.92
	2-way	7553	LP-Guided Greedy	1176.33	1176.33	100.00	1175.33	1175.33	99.91
	2-way	7553	ILP	1175.00	1175.00	100.00	1175.00	1175.00	100.00
	loop	56614	Naive Greedy	727.33	727.67	100.05	730.33	730.33	100.41
	loop	56614	LP-Guided Greedy	725.00	725.00	100.00	725.00	725.00	100.00
	loop	56614	ILP	725.00	725.00	100.00	725.00	725.00	100.00
LDBC	3-split	876933	Naive Greedy	2.00	5.00	250.00	3.33	3.33	166.67
	3-split	876933	LP-Guided Greedy	1.00	2.33	233.33	1.00	1.00	100.00
	3-split	876933	ILP	1.00	2.00	200.00	1.00	1.00	100.00
	1-way	79064	Naive Greedy	22438.00	22438.00	100.00	22438.00	22438.00	100.00
	1-way	79064	LP-Guided Greedy	22438.00	22438.00	100.00	22438.00	22438.00	100.00
	1-way	79064	ILP						
	2-rep	72756	Naive Greedy	42.33	147.33	348.03	59.33	59.33	140.16
	2-rep	72756	LP-Guided Greedy	31.00	67.00	216.13	33.00	33.00	106.45
	2-rep	72756	ILP	31.00	67.00	216.13	33.00	33.00	106.45
LDBC	loop	423	Naive Greedy	48.67	49.00	100.68	50.33	50.33	103.42
	loop	423	LP-Guided Greedy	46.00	46.00	100.00	46.00	46.00	100.00
	loop	423	ILP	46.00	46.00	100.00	46.00	46.00	100.00
	3-split	1358499	Naive Greedy	155.00	149.33	96.34	169.33	169.33	109.25
	3-split	1358499	LP-Guided Greedy	100.00	100.00	100.00	100.00	100.00	100.00
	3-split	1358499	ILP	100.00	100.00	100.00	100.00	100.00	100.00

Table 8: Raw runtimes and runtime comparisons for repairing with sampled errors

Dataset	Shape	#Errors	Algorithm	Base Pipeline		k = 2		k = 4	
				Runtime	Runtime	Runtime Reduction	Runtime	Runtime	Runtime Reduction
Coreutils	1-way	45728	LP-Guided Greedy	113.9463	117.9029	-3.4724	116.1778	-1.9584	
	2-way	3707	LP-Guided Greedy	0.8512	0.8423	1.0449	0.8353	1.8685	
Legislative	1-way	166977	LP-Guided Greedy	111.9393	144.8334	-29.3857	109.1641	2.4792	
	2-way	419439	LP-Guided Greedy						
	loop	3783	LP-Guided Greedy	0.2798	0.1843	34.1506	0.3096	-10.6573	
ICIJ	1-way	558799	LP-Guided Greedy	183.4825	76.8191	58.1328	102.3670	44.2089	
	2-rep	397108	LP-Guided Greedy	45.2682	34.3127	24.2014	83.7004	-84.8988	
	2-way	7553	LP-Guided Greedy	2.3449	2.1603	7.8712	2.3681	-0.9890	
	loop	56614	LP-Guided Greedy	7.5130	4.7326	37.0083	5.4140	27.9375	
LDBC	1-way	876933	LP-Guided Greedy	25.9784	21.9824	15.3820	26.6876	-2.7303	
	2-rep	79064	LP-Guided Greedy	527.7366	524.6183	0.5909	518.9552	1.6640	
	loop	72756	LP-Guided Greedy	3.3646	24.9187	-640.6203	13.4611	-300.0839	
	loop	423	LP-Guided Greedy	0.0140	0.0167	-19.1819	0.0177	-25.9705	

Table 9: Raw edge deletions and deletion comparisons for repairing with sampled errors

Dataset	Shape	#Errors	Algorithm	Base Pipeline		k = 2		k = 4	
				Deletions	Deletions	Percentage	Deletions	Deletions	Percentage
Coreutils	1-way	45728	LP-Guided Greedy	6732.00	6810.33	101.16	6732.00	100.00	
	2-way	3707	LP-Guided Greedy	603.00	603.00	100.00	603.00	100.00	
Legislative	1-way	166977	LP-Guided Greedy	2618.00	3367.33	128.62	2670.00	101.99	
	2-way	419439	LP-Guided Greedy						
	loop	3783	LP-Guided Greedy	38.00	218.00	573.68	92.67	243.86	
ICIJ	1-way	558799	LP-Guided Greedy	1188.33	1245.33	104.80	1204.33	101.35	
	2-rep	397108	LP-Guided Greedy	50.67	630.67	1244.74	207.67	409.87	
	2-way	7553	LP-Guided Greedy	1176.33	1180.67	100.37	1175.67	99.94	
	loop	56614	LP-Guided Greedy	725.00	762.67	105.20	740.33	102.11	
LDBC	1-way	876933	LP-Guided Greedy	1.00	3.00	300.00	3.00	300.00	
	loop	79064	LP-Guided Greedy	22438.00	22582.00	100.64	22443.00	100.02	
	2-rep	72756	LP-Guided Greedy	46.00	57.00	123.91	46.00	100.00	

Table 10: Raw runtimes and runtime comparisons for the scaling experiments for the Coreutils and legislative graphs (1-way constraints)

Dataset and Constraint Shape	#Errors	Algorithm	Base Pipeline		Repair with label deletions (Step 2)	
			Runtime	Runtime Reduction	Runtime	Runtime Increase
Coreutils 1-way	14809	Naive Greedy	26.78	90.68	30.98	115.69
	14809	LP-Guided Greedy	10.78	96.24	12.37	114.76
	14809	ILP	287.15		1245.41	433.72
	19109	Naive Greedy	40.08	88.18	38.56	96.20
	19109	LP-Guided Greedy	12.19	96.41	10.48	86.01
	19109	ILP	339.057		1401.39	413.32
	23393	Naive Greedy	66.43	86.65	64.43	97.00
	23393	LP-Guided Greedy	35.27	92.91	22.94	65.05
	23393	ILP	497.72		2078.88	417.68
	27661	Naive Greedy	93.34	83.36	81.91	87.76
	27661	LP-Guided Greedy	43.98	92.16	22.92	52.12
	27661	ILP	561.02		2352.06	419.25
	35101	Naive Greedy	163.55	80.04	163.26	99.82
	35101	LP-Guided Greedy	56.32	93.13	52.72	93.61
	35101	ILP	819.24		3224.69	393.62
Legislative 1-way	45728	Naive Greedy	290.32	74.86	322.12	110.95
	45728	LP-Guided Greedy	110.73	90.41	105.31	95.11
	45728	ILP	1154.86		timeout	
	26603	Naive Greedy	11.52	84.53	17.28	150.00
	26603	LP-Guided Greedy	4.31	94.21	4.75	110.18
	26603	ILP	74.48		309.06	414.95
	41047	Naive Greedy	26.81	79.30	35.93	134.03
	41047	LP-Guided Greedy	9.81	92.43	8.29	84.55
	41047	ILP	129.51		521.96	403.02
	91841	Naive Greedy	57.60	69.23	85.64	148.67
	91841	LP-Guided Greedy	18.84	89.94	20.37	108.12
	91841	ILP	187.20		766.74	409.57
	98686	Naive Greedy	110.54	70.67	158.43	143.33
	98686	LP-Guided Greedy	43.41	88.48	48.60	111.97
	98686	ILP	376.91		1692.88	449.15
	121968	Naive Greedy	187.30	73.68	258.30	137.91
	121968	LP-Guided Greedy	61.78	91.32	65.68	106.31
	121968	ILP	711.57		3079.11	432.72
	166977	Naive Greedy	356.64	70.10	389.81	109.30
	166977	LP-Guided Greedy	109.13	90.85	98.02	89.82
	166977	ILP	1192.84		timeout	

Table 11: Raw runtimes and runtime comparisons for the scaling experiments for the ICIJ and LDBC graphs (1-way constraints)

Dataset and Constraint Shape	#Errors	Algorithm	Runtime	Base Pipeline		Repair with label deletions (Step 2)	
				Runtime Reduction	Runtime	Runtime	Runtime Increase
ICIJ 1-way	1285	Naive Greedy	0.027	87.97	0.03	100.03	
	1285	LP-Guided Greedy	0.05	78.91	0.09	190.18	
	1285	ILP	0.23		0.54	235.78	
	1517	Naive Greedy	0.17	80.79	0.26	148.87	
	1517	LP-Guided Greedy	0.19	79.20	0.25	135.68	
	1517	ILP	0.89		3.14	351.59	
	2786	Naive Greedy	0.42	94.35	0.58	138.17	
	2786	LP-Guided Greedy	0.31	95.89	0.44	143.73	
	2786	ILP	7.49		28.53	380.64	
	175724	Naive Greedy	36.19	-22.40	66.26	183.08	
LDBC 1-way	175724	LP-Guided Greedy	24.13	18.41	52.79	218.80	
	175724	ILP	29.57		125.52	424.50	
	558799	Naive Greedy	324.12	-445.65	559.79	172.71	
	558799	LP-Guided Greedy	176.13	-196.51	397.95	225.95	
	558799	ILP	59.40		294.69	496.11	
	2052352	Naive Greedy	timeout		timeout		
	2052352	LP-Guided Greedy	timeout		timeout		
	2052352	ILP	timeout		timeout		
	8704	Naive Greedy	14.2085507934292	97.29	25.46	179.22	
	8704	LP-Guided Greedy	8.61	98.36	12.77	148.31	
	8704	ILP	524.46		2402.83	458.15	
	15337	Naive Greedy	54.99	97.12	99.98	181.80	
	15337	LP-Guided Greedy	42.52	97.77	60.18	141.54	
	15337	ILP	1909.62		timeout		
	55957	Naive Greedy	143.65		244.35	170.10	
	55957	LP-Guided Greedy	69.12		92.72	134.14	
	55957	ILP	timeout		timeout		
	79064	Naive Greedy	980.82		1627.58	165.94	
	79064	LP-Guided Greedy	513.14		847.47	165.15	
	79064	ILP	timeout		timeout		

Table 12: Raw number of deletions and comparisons for the scaling experiments of the Coreutils and legislative graphs (1-way constraints)

Dataset and Constraint Shape	#Errors	Algorithm	Base Pipeline		Repair with label deletions (Step 2)	
			#Edge Deletions	Reduction in Deletions	#Label Deletions	Delete Reduction
Coreutils 1-way	14809	Naive Greedy	3679		2579	29.90
	14809	LP-Guided Greedy	2763.67	24.87	2092.00	24.30
	14809	ILP	2754	25.14	2092	24.04
	19109	Naive Greedy	4115		2655	35.49
	19109	LP-Guided Greedy	2848.33	30.79	2092.00	26.55
	19109	ILP	2824	31.38	2092	25.92
	23393	Naive Greedy	5207		3299	36.65
	23393	LP-Guided Greedy	4107.33	21.12	2586.67	37.02
	23393	ILP	4069	21.86	2586	36.45
	27661	Naive Greedy	5753		3344	41.87
	27661	LP-Guided Greedy	4346.00	24.46	2586.67	40.48
	27661	ILP	4257	26.00	2586	39.25
	35101	Naive Greedy	6870		4344	36.77
	35101	LP-Guided Greedy	5095.33	25.84	3375.00	33.76
	35101	ILP	5088	25.94	3375	33.67
Legislative 1-way	45728	Naive Greedy	8747		5657	35.33
	45728	LP-Guided Greedy	6732.00	23.04	4462.00	33.72
	45728	ILP	6732	23.04	timeout	
	26603	Naive Greedy	1003		630	37.21
	26603	LP-Guided Greedy	762.00	24.05	370.00	51.44
	26603	ILP	762	24.05	370	51.44
	41047	Naive Greedy	1551		760	50.98
	41047	LP-Guided Greedy	1082.00	30.24	441.00	59.24
	41047	ILP	1082	30.24	441	59.24
	91841	Naive Greedy	1830		1012	44.70
	91841	LP-Guided Greedy	1365.00	25.41	596.00	56.34
	91841	ILP	1365	25.41	596	56.34
	98686	Naive Greedy	2421		1390	42.59
	98686	LP-Guided Greedy	1797.00	25.76	774.00	56.93
	98686	ILP	1797	25.76	774	56.93
	121968	Naive Greedy	3185		1695	46.78
	121968	LP-Guided Greedy	2100.00	34.06	899.00	57.19
	121968	ILP	2100	34.06	899	57.19
	166977	Naive Greedy	3819		1905	50.10
	166977	LP-Guided Greedy	2618.00	31.44	1064.00	59.36
	166977	ILP	2618	31.44	timeout	

Table 13: Raw number of deletions and comparisons for the scaling experiments of the ICIJ and LDBC graphs (1-way constraints)

Dataset and Constraint Shape	#Errors	Algorithm	Base Pipeline		Repair with label deletions (Step 2)	
			#Edge Deletions	Reduction in Deletions	#Label Deletions	Delete Reduction
ICIJ 1-way	1285	Naive Greedy	55		39	28.05
	1285	LP-Guided Greedy	44.33	18.90	38.00	14.29
	1285	ILP	43	21.34	38	11.63
	1517	Naive Greedy	186		167	10.38
	1517	LP-Guided Greedy	176.00	5.55	149.33	15.15
	1517	ILP	174	6.62	149	14.37
	2786	Naive Greedy	338		261	22.88
	2786	LP-Guided Greedy	261.33	22.68	226.33	13.39
	2786	ILP	260	23.08	226	13.08
	175724	Naive Greedy	753		581	22.92
	175724	LP-Guided Greedy	627.67	16.68	476.00	24.16
	175724	ILP	616	18.23	463	24.84
	558799	Naive Greedy	1411		1008	28.54
	558799	LP-Guided Greedy	1188.00	15.80	826.00	30.47
	558799	ILP	1188	15.80	807	32.07
LDBC 1-way	2052352	Naive Greedy	timeout		timeout	
	2052352	LP-Guided Greedy	timeout		timeout	
	2052352	ILP	timeout		timeout	
	8704	Naive Greedy	5782		5441	5.89
	8704	LP-Guided Greedy	4854.00	16.045	4711.00	2.95
	8704	ILP	4854	16.04	4711	2.95
	15337	Naive Greedy	11304		10318	8.72
	15337	LP-Guided Greedy	10227.00	9.52	8978.00	12.21
	15337	ILP	10227	9.52	timeout	
	55957	Naive Greedy	12829		11486	10.47
	55957	LP-Guided Greedy	11339.00	11.62	9732.00	14.17
	55957	ILP	timeout		timeout	
	79064	Naive Greedy	22438		21099	5.97
	79064	LP-Guided Greedy	22438.00		19740.00	12.02
	79064	ILP	timeout		timeout	

Table 14: Runtimes for computing repairs with custom weights (PageRank scores)

Dataset	Shape	#Errors	Algorithm	Runtime	Runtime Increase	Edge Deletions	Deletion Reduction
ICIJ	1-way	558799	Naive Greedy	439.04	-1655.31	2643.00	
	1-way	558799	LP-Guided Greedy	185.26	-640.69	1266.00	52.10
	1-way	558799	ILP	25.01		1264.00	52.18
	2-rep	397108	Naive Greedy	212.25		153.00	
	2-rep	397108	LP-Guided Greedy	40.14		73.00	52.29
	2-rep	397108	ILP				
	2-way	7553	Naive Greedy	4.30	-693.78	1912.00	
	2-way	7553	LP-Guided Greedy	2.43	-349.08	1189.67	37.78
	2-way	7553	ILP	0.54		1188.00	37.87
	loop	56614	Naive Greedy	7.32	-312.05	732.00	
	loop	56614	LP-Guided Greedy	7.63	-329.29	726.00	0.82
	loop	56614	ILP	1.78		726.00	0.82
Coreutils	3-split	876933	Naive Greedy	14.79	45.80	2.00	
	3-split	876933	LP-Guided Greedy	26.10	4.39	1.00	50.0
	3-split	876933	ILP	27.29		1.00	50.0
	1-way	45728	Naive Greedy	250.91	-13373.86	8595.00	
	1-way	45728	LP-Guided Greedy	103.88	-5478.28	6737.00	21.62
	1-way	45728	ILP	1.86		6737.00	21.62
Coreutils	2-way	3707	Naive Greedy	1.57	-473.44	786.00	
	2-way	3707	LP-Guided Greedy	1.13	-310.75	751.00	4.45
	2-way	3707	ILP	0.27		708.00	9.92

Table 15: Runtimes for computing approximate repairs for the selection phase of the naive greedy (NG) and LP-guided greedy (LPG)

Dataset	Shape	#Errors	Algorithm	Runtime
Coreutils	1-way	45728	Approximate NG	0.38
	1-way	45728	Approximate LPG	1.39
	2-way	3707	Approximate NG	0.04
	2-way	3707	Approximate LPG	0.10
Legislative	1-way	166977	Approximate NG	1.69
	1-way	166977	Approximate LPG	3.99
	2-way	443695	Approximate NG	timeout
	2-way	443695	Approximate LPG	timeout
	loop	3783	Approximate NG	0.14
	loop	3783	Approximate LPG	0.23
ICIJ	1-way	558799	Approximate NG	11.15
	1-way	558799	Approximate LPG	20.11
	2-rep	397108	Approximate NG	7.41
	2-rep	397108	Approximate LPG	19.72
	2-way	7553	Approximate NG	0.08
	2-way	7553	Approximate LPG	0.22
	loop	56614	Approximate NG	0.93
	loop	56614	Approximate LPG	1.68
	3-split	876933	Approximate NG	15.69
	3-split	876933	Approximate LPG	26.00
LDBC	1-way	79064	Approximate NG	0.63
	1-way	79064	Approximate LPG	2.77
	2-rep	72756	Approximate NG	1.32
	2-rep	72756	Approximate LPG	2.37
	loop	423	Approximate NG	0.00
	loop	423	Approximate LPG	0.01
	3-split	1358499	Approximate NG	22.32
	3-split	1358499	Approximate LPG	51.70

Table 16: Edge deletions of approximate repairs suggested by the selection phase of the naive greedy (NG) and LP-guided greedy (LPG)

Dataset	Shape	#Errors	Algorithm	Runtime
Coreutils	1-way	45728	Approximate NG	11820.67
	1-way	45728	Approximate LPG	6733.67
	2-way	3707	Approximate NG	744.33
	2-way	3707	Approximate LPG	603
Legislative	1-way	166977	Approximate NG	5483.33
	1-way	166977	Approximate LPG	2618
	2-way	443695	Approximate NG	
	2-way	443695	Approximate LPG	
	loop	3783	Approximate NG	87
	loop	3783	Approximate LPG	38
ICIJ	1-way	558799	Approximate NG	1580.33
	1-way	558799	Approximate LPG	1188
	2-rep	397108	Approximate NG	113.67
	2-rep	397108	Approximate LPG	92
	2-way	7553	Approximate NG	1743.33
	2-way	7553	Approximate LPG	1180
	loop	56614	Approximate NG	731.67
	loop	56614	Approximate LPG	725
	3-split	876933	Approximate NG	9.67
	3-split	876933	Approximate LPG	1
LDBC	1-way	79064	Approximate NG	30464.33
	1-way	79064	Approximate LPG	22438
	2-rep	72756	Approximate NG	95.33
	2-rep	72756	Approximate LPG	31
	loop	423	Approximate NG	51.33
	loop	423	Approximate LPG	46
	3-split	1358499	Approximate NG	311.67
	3-split	1358499	Approximate LPG	100